How multiscale curvature couples forces to cellular functions

Marine Luciano, Caterina Tomba, Aurélien Roux, Sylvain Gabriele

https://doi.org/10.1038/s42254-024-00700-9

How multiscale curvature couples forces to cellular functions

Marine Luciano[1], Caterina Tomba[2], Aurélien Roux[1,3] & Sylvain Gabriele[4]

Abstract

Among the physicochemical cues in the cellular microenvironment that orchestrate cell processes, the different levels of curvature in the extracellular matrix and intrinsic to the tissues play a pivotal role in the spatiotemporal control of key cellular functions. Curvature influences multicellular organization and contributes to the onset of specific human diseases. This Review outlines how physical parameters used to describe the balance of forces in cells and tissues shed light on the mechanism of curvature sensing of cells across different length scales. We provide a summary of progress in delineating the fundamental mechanobiological characteristics of curvature sensing across various scales, emphasizing key challenges in the field. Additionally, we explore the potential of vertex model approaches to uncover critical physical elements involved in the mechanical regulation of curved tissues and the construction of functional architectures at the collective level. Finally, we examine how changes in curvature can influence transcriptional regulation through a reorganization of cytoskeletal forces acting on the nucleus, thereby facilitating the development of specific human diseases.

Sections

[1]Department of Biochemistry, University of Geneva, Geneva, Switzerland. [2]CNRS, INSA Lyon, Ecole Centrale de Lyon, Universite Claude Bernard Lyon 1, CPE Lyon, INL, UMR5270, Villeurbanne, France. [3]National Center of Competence in Research in Chemical Biology, University of Geneva, Geneva, Switzerland. [4]Mechanobiology & Biomaterials Group, Research Institute for Biosciences, CIRMAP, University of Mons, Mons, Belgium. e-mail: sylvain.gabriele@umons.ac.be

Key points

- Cells interact with the curved surfaces of many organs and, at a lower scale, with the rounded features of the extracellular matrix, which inherently links geometric form and biological function.
- The curvature of the extracellular matrix influences vital cellular processes by defining physical boundary conditions across multiple scales.
- Multicellular tissues are active materials, and curved patterns in tissues emerge from stress fields generated by intrinsic forces coupled with extrinsic constraints.
- The regulation of cellular shape and tension by curvatures at various length scales activates specific mechanotransduction pathways that synergistically determine downstream cellular functions.
- Changes in the balance of cellular forces required to adapt to curved environments can have dramatic consequences, promoting the emergence of various human diseases.

Introduction

Curved surfaces are a hallmark of many biological tissues, enabling important functions such as maximizing the surface-to-volume ratios. Examples include brain gyri that optimize neuronal connectivity[1], intestinal villi that enhance nutrient absorption in the gut, and alveoli that facilitate gas exchange in the lungs. Interestingly, cells not only interact with micrometre-scale curved features but also with the curved nanostructures of the extracellular matrix (ECM), reshaping their membrane and cytoskeletal components accordingly.

In addition to other physical ECM cues such as stiffness[2–4], confinement[5–7], viscoelasticity[8–10] or mechanical stretch[11–14], growing evidence suggests that the length scale of curved features substantially influences cellular and tissue functions, guiding repair mechanisms, tissue morphogenesis and pathological processes[15–19]. Moreover, there is an intricate relationship among biological form, function and mechanical forces[20]; it is thus important to study how cells and tissues adapt to curved nanoenvironment and microenvironment with a specific response in terms of force balance. Investigating the interplay among shape, force and cell regulation in response to modifications of the cell microenvironment properties has laid the foundations for cell mechanobiology as a discipline[21]. Among other physical ECM cues, how curvature of the cell microenvironment affects the interplay between cell shape and force is crucial for understanding the organization, dynamics and fate of individual cells and collectives.

We present an overview of the impact of curvature at different length scales on cell organization, motility and morphogenesis. We describe the coupling of cell forces and shapes to curvature. We also show how cell shape adapts to the matrix curvature and we discuss vertex models used to determine the balance of forces in the emergence of curved patterns. Finally, we highlight the importance of understanding the cellular and tissue responses to substrate curvature, as they hold insights into the complex mechanisms involved in various pathological conditions and diseases associated with matrix curvature.

Forces and tissue curvature generation

The human body is characterized by geometric and topological structures that exhibit curvatures ranging from the molecular to the organ scale (Box 1). In 2D, curvature is represented by a curved line in the plane (*xy*), whereas in the perpendicular dimensions (*xz* and *yz*), the line forms an out-of-plane (3D) curved surface (Box 2). Within living systems, the environment is primarily 3D and highly structured, influenced by Gaussian and mean curvature distributions that give rise to numerous complex structures (Box 2). Curvature manifests at the microscopic level within organs and extends to the organs themselves, relying on a modulation of the balance of forces generated by various sources.

Balance of forces in the emergence of curved patterns

Multicellular tissues are active materials composed of force-generating, growing and dividing cells. As for any material, their deformation depends on the force balance applied to them. But the tissue forces can be intrinsic, generated by the cells themselves, or external, or can result from a combination of active cell processes (growth and proliferation) and external constraints (pressure and spatial confinement). We review the different intrinsic forces within tissues and describe how forces are combined with extrinsic constraints to generate stress fields that can shape tissues. Tissue-intrinsic forces emerge from subcellular forces that integrate over multicellular distances through multicellular features such as cell–cell adhesion, order and tissue fluidity.

Intrinsic forces at the single-cell level. Active cells generate three types of forces: osmotic pressure, cytoskeleton forces and membrane tension (Fig. 1a). These forces are not independent, as changes in one also affect the value of others.

Cells are delimited by a semi-permeable lipid membrane. Thus, any concentration change of solutes across the cell membrane changes the cell osmotic pressure, and active pumping of solutes across the membrane may create osmotic gradients. The osmotic pressure inside cells varies from cell type to cell type and is particularly high in organisms having a cell wall and growing through turgor pressure[22]. In the first approximation of a spherical cell, the osmotic pressure of the cell is coupled to its volume through the Laplace law ($P = \frac{2\sigma}{R}$, in which P is the pressure, σ is the membrane tension (discussed subsequently) and R is the radius). Experimentally, it is found that the volume of cells is coupled to its osmotic pressure, but with a minimal, incompressible volume, leading to the Ponder–Boyle–Vant'Hoff equation that accounts for changes of volume with changes of osmotic pressure ($P(V - V_{0I}) = P_0(V_0 - V_{0I})$), in which P and V are the osmotic pressure and volume after the volume change, P_0 and V_0 are the osmotic pressure and volume before the osmotic change and V_{0I} is the minimal (osmotically inactive) volume. However, the complex dynamics of the osmotic response under hypotonic shocks modifies this relation between volume and pressure in times longer than a few tens of seconds[23]. In multicellular tissues, the turgor pressure is an integration of the different osmotic pressures of its cells and can generate a pressure when the tissue is under confinement. Importantly, many tissues have also liquid cavities between cells, and osmotic pressure is regulated by ions pumped by cells within the cavity. In this case, the pressure of the cavity applies to the cells, which can participate in tissue deformation[24]. Three ionic transporters participate in balancing the osmotic pressure between the cell and its external media[25]. As these transporters are regulated genetically and biochemically, different levels of osmotic pressure are obtained through different regulations.

Box 1

Scales of curvature in the human body

In living systems, curvature is a prevalent characteristic observed within the extracellular matrix (ECM) and organs. The human body has a range of curved structures spanning various length scales (see the figure, part **a**) in both 2D and 3D[15,19,188–192].

At the subcellular scale, curved structures are found in the ECM, which comprises fibrillar proteins and proteoglycans. For instance, mature tendons exhibit collagen fibrils of few hundreds of nanometres in diameter, forming bundles spanning tens to hundreds of micrometres[193] (see the figure, part **b**). Curved ECM fibres arise from a reciprocal feedback between ECM fibres and cells[194], and aligned collagen networks are observable in specific tissues by using second harmonic generation microscopy (see the figure, part **c**). Specific cell types, such as fibroblasts, actively participate in the alignment process of collagen fibres, thereby enhancing the migratory persistence of tumour cells[195]. Within bones, a highly curved hierarchical structure is formed, encompassing collagen fibrils, osteons and osteocytes. Osteons are cylindrical structures of mineral matrix of diameter 100–200 µm that permit living osteocytes to align with the bone axis[196] (see the figure, part **d**).

Curvature at the subcellular scale is not only associated with the ECM but also intrinsic to the cell itself. Notably, the lipid bilayers of the cell membrane can form either convex surfaces, forming membrane-bound vesicles with diameters ranging from tens to hundreds of nanometres, or concave shapes with cleavage furrows during cytokinesis, characterized by a ring of diameter 1–2 µm. Moreover, cellular extensions known as cilia and flagella, with diameters in the range of tens to hundreds of nanometres, are present in various microorganisms and eukaryotic cells to facilitate movement or guide their motion through fluids. The twist of bundles of microtubule filaments in the axoneme, the inner motile structure of cilia and flagella, is crucial for regulating the motion of the motors, enabling the production of coordinated waveforms and serving as mechanism through which motors can sense curvature[197]. Highly curved protrusions are also observed in the microvilli, ~100 nm in diameter, enhancing the apical surface area for absorption in epithelial cells of the small intestine. Within cells, multifolding structures give rise to the Golgi apparatus and the endoplasmic reticulum, characterized by spirals and tubules with diameters of

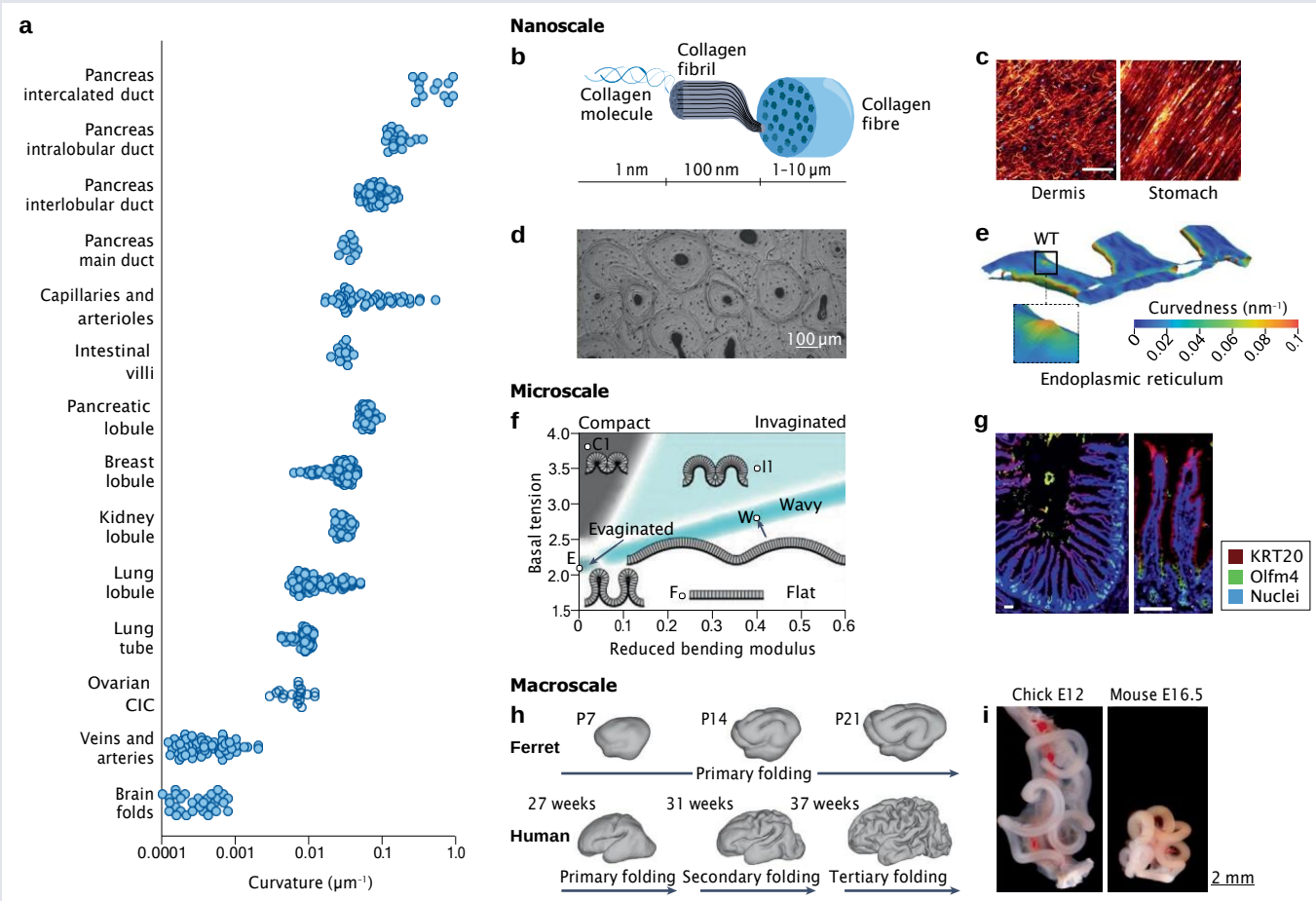

(continued from previous page)
a few tens of nanometres[198,199], and peaks of curvature measuring <10 nm[200] (see the figure, part **e**).

On a larger scale, epithelial cells line the interior surface of cylindrical or lobular structures in various organs, including the lung, kidney, breast and pancreas. Epithelial tissues from different organs, such as the urinary bladder and skin, exhibit folds at varying dimensions, which can be attributed to common mechanisms driven by physical forces[63,201]. Apical constrictions are integral to developmental processes, involving the active narrowing of cellular apices[202] and the local reduction of basal tension owing to decreased ECM density, along with increased lateral tension resulting from F-actin fluctuations[203,204] (see the figure, part **f**). In the intestinal barrier, chemical gradients contribute to maintaining cell compartmentalization within the villus-crypt structure[205] (see the figure, part **g**), and tension gradients facilitate compartmentalization, folding and collective migration[52]. The highly curved organization of the gastrointestinal tract has mechanical origins[206] linking morphogen-based patterning and muscle alignment[207], whereas the brain undergoes progressive cortical folding stages driven by mechanical forces[208] (see the figure, part **h**). Finally, curved macrostructures could also be observed in the human body, as in the veins and arteries of the cardiovascular system or the looping pattern of the gut (see the figure, part **i**).

Part **c** is reprinted with permission from ref. 194, CC BY 4.0. Part **d** reprinted with permission from ref. 196, Elsevier. Part **e** reprinted with permission from ref. 200, Elsevier. Part **g** reprinted with permission from ref. 205, Elsevier. Part **h** reprinted with permission from ref. 208, Royal Society. Part **i** adapted from ref. 206, Springer Nature Limited.

One manifestation of cytoskeleton forces is the cell contractility that is generated by protein filaments, actin, onto which myosin molecular motors can exert forces. Myosins are chemo–mechanical transduction machines that operate via the rotation of their lever arm in response to actin binding and ATP hydrolysis[26]. Motors can move actin filaments relative to each other, leading to contraction, but a part of the contractile forces is generated by the constant polymerization–depolymerization dynamics of actin fibres. Depending on how the actin filaments are organized, how they are bound to the membrane and/or crosslinked, the actomyosin system can form contractile rings during cell division, stress fibres to anchor cells onto a substrate or a contractile surface known as lamellipodia for cell migration. In most cells, a thin contractile layer tightly bound to the plasma membrane, known as the actin cortex, keeps cells under tension.

Another source of cytoskeleton forces is microtubules. Forces implicated in tissue remodelling and the formation of curved patterns are not exclusively attributed to the actomyosin network but can also stem from microtubules. The polymerization of microtubules involves the addition of a GTP–tubulin dimer, corresponding to a mechanical force of approximately 4 pN (ref. 27). The polymerization or depolymerization of a single microtubule composed of 13 protofilaments can generate a force of approximately 50 pN (ref. 28). Additionally, microtubules can interact with molecular motors to generate pushing or pulling forces, which are crucial for creating stress fields that shape tissues[29]. An active role of microtubules in generating compressive forces to stabilize cell shape during morphogenesis has been uncovered in *Drosophila*. Further research is needed to understand the contribution of microtubules and other cytoskeletal components, such as vimentin, to the generation of shaping forces in epithelial tissues.

Finally, various definitions of membrane tension have been proposed[30], starting with the original thermodynamic definition[31]. We adopt a mechanical definition, wherein membrane tension is considered to be the reactive force in response to the stretch of a lipid membrane. Through the Laplace law, osmotic pressure has a direct contribution to membrane tension. The actomyosin system also has a direct contribution to membrane tension, mostly through cortical actin contractility, but also through the protrusion of filopodia and lamellipodia. Other processes can regulate membrane tension: endocytosis and exocytosis that regulate membrane area; the formation of caveolae, which are plasma membrane invaginations that buffer rapid increase in tension; or lipid metabolism. The actomyosin cortex and osmotic pressure are thus coupled in the regulation of cell surface tension, all of which participate in processes of many cells. For example, in migrating cells, there is a gradient of membrane tension, coupled to the actin dynamics[32–35]. But the cellular process in which the balance between osmotic pressure, actin cortex contractility and membrane tension is the most appreciable is probably cell division. During cytokinesis, changes in the composition and structure of the contractile actomyosin cortex, along with osmotic swelling, lead to substantial modifications in cell morphology. These morphological modifications allow a dividing cell to generate force against its surroundings[36]. Moreover, a complex mechanical feedback loop activates the cortical actin contractility if one of the daughter cells gets too large, avoiding the smaller cell emptying itself into the larger one because of an instability created by differences in osmotic pressure[37].

All these forces contribute to the collective forces that shape curved tissues, but additional properties of collective assemblies must also be considered.

Combining intrinsic forces at the multicellular level. Additional properties associated with multicellularity are essential to integrate forces over multicellular distances: cell–cell adhesion and cell–substrate adhesion, cell planar polarity and cell order.

Intercellular interactions are usually mediated by cadherin-like molecules. Cadherins have many isoforms, but usually the adhesive force they provide is strongest between cells expressing the same isoform (isoforms) at their surface. In epithelial cells, cadherins form a more structured adhesive zone called the adherens junction. Adherens junctions in epithelial cells are located on their apical side and are linked to an actomyosin ring that participates in keeping cell under lateral tension (Fig. 1b). Thus, the adherens junctions are linked to the contractile machinery of the cells that propagates tension over large distances, which is also true for any cells interacting through cadherins.

Another essential adhesive property of cells is their adhesion to the substrate. Usually, ECM proteins interact with integrins. Integrins are transmembrane proteins bound to the actin–cytoskeleton in the cell (Fig. 1b). They are part of focal adhesions, structures known to provide strong anchoring of cells to stiff substrates. Focal adhesions are also essential actors of the mechanosensing pathways.

Planar cell polarity is associated with an anisotropic shape of the epithelial cells, and the localization of specific proteins, in particular

Box 2

Geometrical concepts of curvature

To understand the effect of curvature on cells and tissues, it is first necessary to define the term and the main geometries associated with curved surfaces. In the context of surfaces, the curvature can be defined by considering two principal curvatures, denoted as k_1 and k_2, also referred to as maximum and minimum curvature, respectively (see the figure, part **a**). These curvatures correspond to the inverse of the radius of a circle that is tangential to the surface at the corresponding point (see the figure, part **b**). Curved surfaces can also be classified as concave when they curve inward or as convex when they curve outwards (see the figure, part **b**). A concave surface and a convex surface with identical curvatures fit perfectly into each other.

Taking the example of a cylinder, which is a surface with constant curvature, k_1 represents the maximum curvature along the axis of the cylinder, indicating the rate at which the surface curves in the direction of its length. Conversely, k_2 represents the minimum curvature, indicating the rate of curvature in the direction perpendicular to the length of the cylinder. Together, k_1 and k_2 provide a complete description of how the surface curves at a specific point, offering valuable insights into its geometric properties. The product of the two principal curvatures ($K = k_1k_2$) defines the Gaussian curvature (K), which is a quadratic term. The average of the two principal curvatures determines the mean curvature (H), $H = (k_1 + k_2)/2$. K is an intrinsic measure defined by the surface itself, whereas H is an extrinsic measure determined by the surface and its surrounding[209]. Therefore, it does not characterize the shape but gives the amount of curvature in one way or another. The intrinsic property of curvature does not depend on the embedding of the surface, whereas the extrinsic does. This is best reflected in the fact that when integrated over the whole surface, Gaussian curvature is a constant, the value of which depends on the topology of the surface and not its shape, whereas the integral of H varies markedly as a function of the global shape of the surface. According to the Gauss-Bonnet theorem, the integral of K over the entire manifold with respect to area is 2π times the Euler characteristic of the manifold ($\int K ds = 2\pi\chi$, in which χ is Euler's characteristic). An infinite flat surface has K and H values of zero, as both k_1 and k_2 are zero (see the figure, part **c**). Infinite cylindrical surfaces obtained through isometric folding have one principal curvature equal to zero, resulting in $K = 0$ at any point (green dotted line; see the figure, part **c**). Structures such as domes and spheres have non-zero values for both k_1 and k_2, exhibiting curvature in a consistent direction and consequently have a positive K (orange dotted line). Saddle-like surfaces or branched tubes exhibit principal curvatures (k_1 and k_2) curving in opposite directions and not equal to zero, leading to a negative K (blue dotted line). The situation differs for H because it depends on how the surface is incorporated in the surrounding 3D environment and, therefore, the chosen direction for the normal surface.

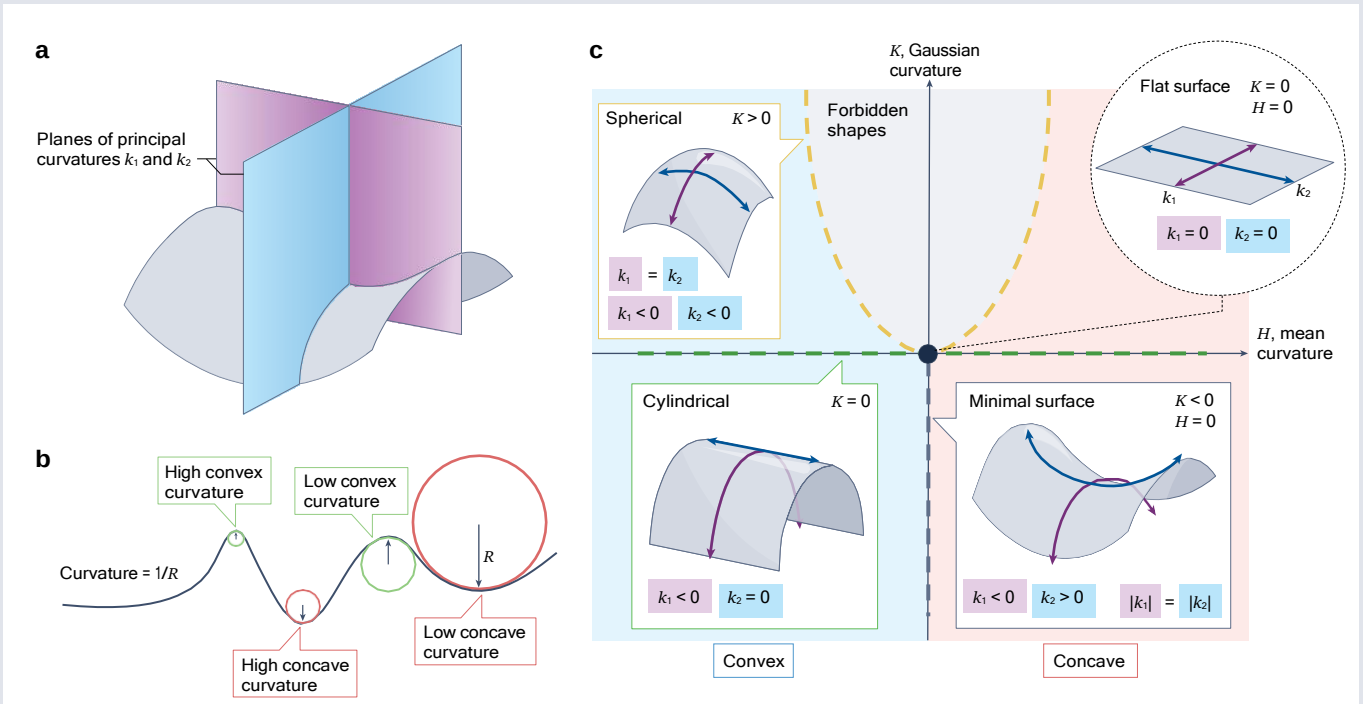

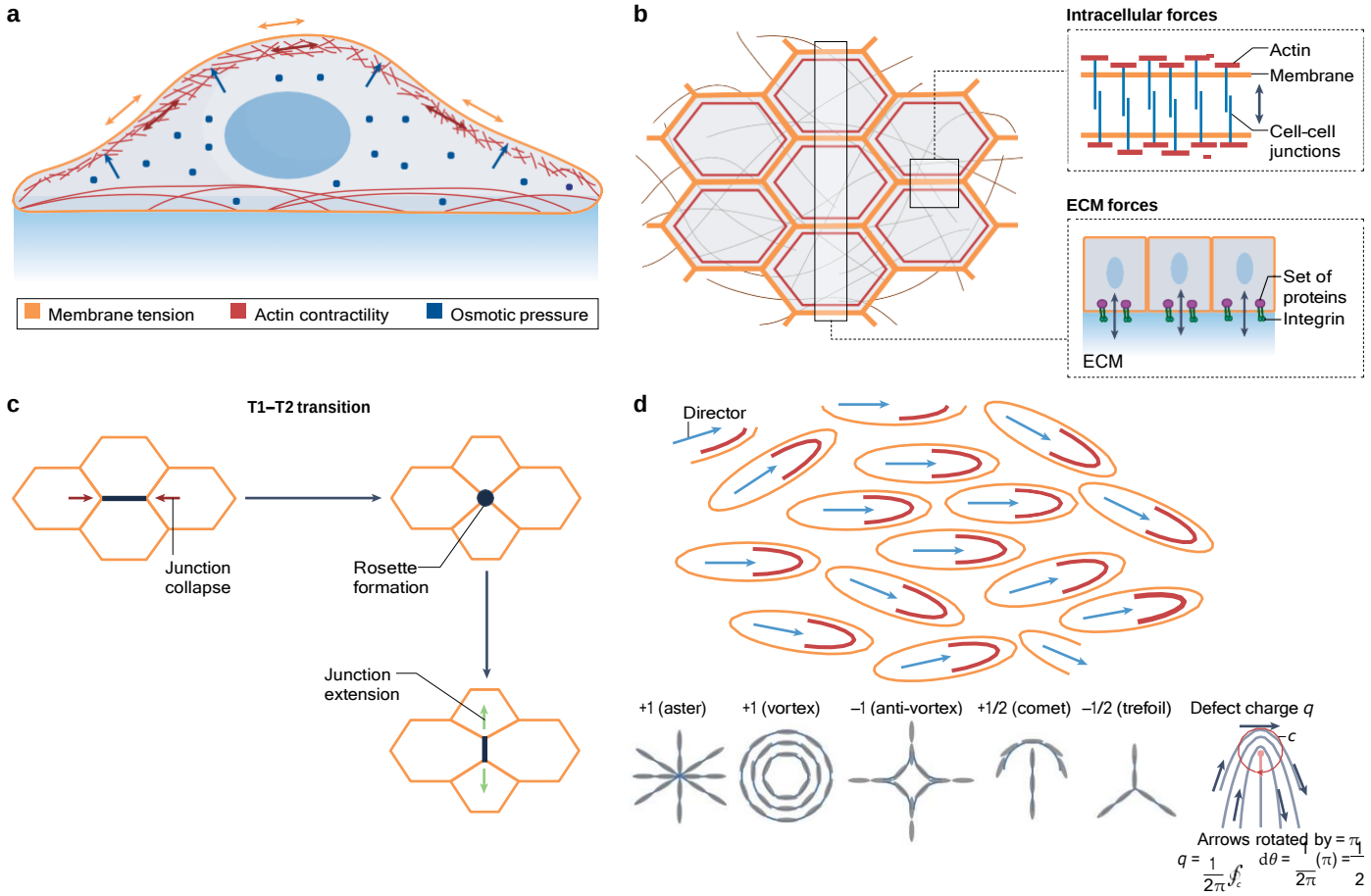

Fig. 1 | Forces acting at the tissue scale. a, Forces at the single-cell level include membrane tension, actin contractility and osmotic pressure. **b**, Epithelial cells can assemble into cohesive monolayers where individual cells adopt a polygonal shape (normal view). Cells interact with each other through adhesive interactions such as cadherins, and with the substrate via transmembrane proteins such as integrins. **c**, In epithelia, coordination of contractility in a small group of cells leads to T1–T2 transition. **d**, At a larger scale, cohesive cell assemblies can be described by their nematic order of single-cell directors (the orientational vector of the cells). Nematic order forms lines of order organized by topological defects (grey schematics) and coordinates the motility and contractility of cells at the tissue scale. ECM, extracellular matrix. Part **d** adapted with permission from ref. 186, Elsevier.

adhesion molecules and actomyosin components, at one or several poles of the cell. These anisotropies can orient all forces into one direction, leading to cell motion towards a main direction. Such orientation occurs in the case of T1–T2 transitions (Fig. 1c), which are driven by cell planar polarities that push one row of cells in a hexagonal lattice of epithelial cells to intercalate in between the cells of a neighbouring row. These intercalations generate shearing flows that cause the tissue to expand predominantly in one direction while concurrently reducing its length in the perpendicular direction[38].

Finally, dense assemblies of anisotropic cells can produce an orientational field that is described by a nematic order and is coupled to the collective flow field of cells[39] (Fig. 1d). One essential difference between collective cell migration and liquid crystals is that cells are active and produce their own forces, forming multicellular flows similar to the ones observed in thin layers of dense cytoskeleton filaments and motors[40]. Following Newton's principle, these flows are created by spatiotemporally varying stress fields, which are organized by topological defects. Understanding how assemblies of cells interact to create active stress fields that generate flows is a growing subject of interest to understand morphogenesis, as these stress fields are expected to be the ones shaping tissues. In passive nematic systems at rest, the order tends to homogenize in one direction (Fig. 1d, top). In active systems, because of the varying force field, there is a constant rate of creation of nematic defects, which are points where the order is lost. These defects are surrounded by specific patterns of orientational and velocity fields, which define their topological charge (Fig. 1d, bottom). Because of the specific orientational and flow field around them, defects impose structure in the gradients of forces around them[41]. These gradients can be contractile, meaning that the defects are under compressive forces, or extensile, meaning that defects are under stretching forces[42,43]. Whether stresses around defects are contractile or extensile depends on several factors: the balance between motility and contractility, but also cell–cell adhesion. For example, reducing the expression of proteins involved in establishing adhesive interactions between epithelial cells transforms contractile stress fields around defects into extensile stress fields[44].

Mechanisms of tissue curvature generation

All mechanisms by which tissues can deform and generate curvature involve forces. To unveil these mechanisms, one must measure these forces at various scales. In addition to using various biological model systems for studying in vivo tissue curvature generation, scientists have adopted a reconstitution approach that mimics key stages of morphogenesis and allows the measurement of forces under standardized conditions.

Hydrostatic and osmotic pressure. Many embryos and tissues grow and deform around liquid cavities, which are created by osmotic fracturing[45]. In vitro, epithelia recapitulate some features of osmotic deformation. Epithelia are osmotic barriers to protect tissues from their osmotically varying environment. These cells actively pump ions to maintain their osmotic pressure regardless of environmental changes. When Madin–Darby canine kidney epithelial cells cover a small, flat micropattern onto which they weakly adhere, a liquid cavity forms between the epithelium and the substrate[24]. Because of active ion pumping, the cavity osmotically swells, forming growing domes of cells. When their contractility opposes their osmotic stretch, most of the cells flatten, some more than others: certain cells acquire superelastic properties to accommodate the large tissue deformation induced by osmotic swelling[46]. This mechanical behaviour enables epithelial tissues to sustain several-fold areal strains under constant tension leading to a curved epithelium enclosing a pressurized lumen. These observations recapitulate osmotic swelling seen in mouse embryos, in which periodic swelling occurs once the liquid cavity of the blastula has been formed[47].

Apical constriction. Apical constriction is probably the most ancient mechanism discovered that causes multicellular curvature generation[48,49]. Epithelial (ectodermal for embryos) cells are polarized and some of them exhibit a higher contractility at their apical side, which leads to curvature of the tissue, a mechanism essential to fold the ectoderm during gastrulation of all animals. Apical constriction was experimentally demonstrated in the 1930s when it was observed that the gastrula plate of sea anemones — the half of the embryo containing the animal pole — could still invaginate even after dissection[49]. Further discoveries provided robust support for this mechanism by reporting the presence of contractile actin filaments at the apical side of epithelial cells[50]. Furthermore, many simulations recapitulating apical constriction, including vertex models, predict correctly the shapes of different gastrulating embryos[51]. The most recent achievements have measured the forces generated by apical constriction during the formation of crypts in intestinal organoids[52,53]. Interestingly, these stresses are not very strong (maximum 50 Pa)[52] but their impact on curvature is enhanced when combined with cell elongation[54,55]: if cells subjected to apical constriction get thicker, the resulting curvature is larger. Therefore, the balance between lateral and apical tension is critical in setting the curvature of epithelial tissues.

However, apical constriction is probably not sufficient for gastrulation: attachment to the eggshell in gastrulating insect embryos is essential for generating the cell flows required for deep invagination[56,57]. Attachment and confinement provided by the eggshell may enable other multicellular forces to apply. Thus, a two-step mechanism could be proposed: the initiation of gastrulation could be controlled in time and space by inducing apical constriction at the appropriate timing and location. If apical constriction fails to generate sufficient forces for further propagating the invagination, substantial forces at the tissue scale are required. Compression-inducing buckling or large ordered flows could be the final driving forces of gastrulation.

Buckling of epithelia. When apical constriction was discovered, one of the competing hypotheses was buckling: as all embryos grow in eggshells, confinement could lead to accumulation of compressive stresses that could be relaxed by buckling, forming the primordial invagination of gastrulation. Buckling is a simple mechanical process, in which anisotropic elastic material under compression prefers to bend rather than elastically compressing. Theoretical models can easily predict the formation of epithelial folding by buckling[58–60]. Because buckling is a global force-dependent mechanism, showing that the invagination is formed through buckling requires measurement of compressive stresses within the embryo, which remains technically challenging. An in vitro approach makes it possible to reconstitute the geometry of the embryo by encapsulating proliferating epithelia in hollow spheres of alginate[61] (Fig. 2a). In these elastic shells, epithelial cells, adhering to the inner surface of the capsule, form a spherical cell layer that proliferates, accumulating compressive stresses. At pressures in the range of 100 Pa, measured by the elastic expansion of the capsule, the epithelium buckles and invaginates.

Interestingly, in the real embryo, confinement could be achieved by other means than having an elastic eggshell: confinement could come from tissues with low proliferation surrounding tissues with high proliferation. Such confinement occurs in the formation of drosophila wing veins[62], which buckle out of the wing plane by proliferating more than surrounding tissues. Notably, in cellular aggregates in vitro, a different mechanism for buckling leads to complicated folding patterns analogous to Miura origami structures with a four-fold vertex pattern, similar to those observed in the chick embryo[63]. The necessary strain to form these tessellated curvature motifs, consisting of three concave folds and one convex fold, is generated by stresses induced by non-muscle myosin II molecular motors. This process leads to local ECM compaction and alignment of nearby collagen fibres.

Nematic defects organize tissue morphogenesis. Collective flows of cells are organized by cell nematic order, and topological defects could thus organize large scale stress fields that could shape tissues (Fig. 2b). In unconfined cell monolayers, however, only defects with no circular symmetry are observed (+1/2 and −1/2 defects). +1 Defects (concentric circles, spirals and asters) have circular symmetry and thus potentially can concentrate large stresses. But how are integer defects created? Cells collectively migrating on a ring pattern always exhibit rotational movements, with a defined chirality depending on the cell type[64]. But in rings, the defect is materialized by the absence of cells in the centre of the disc. Could cell form integer defects on their own, and create larger stresses? On discoidal micropatterns smaller than the spontaneous inter-defect length, highly nematic muscle cells initially form spirals. These spirals form domes while cells continue to proliferating, the spiral transforming into a vortex that grows into a rotating cylinder, alike a tornado[65]. Because the force fields within the spirals and the tornadoes are compressive, the rotating nematic flow of cells constrains the growth within a cylindrical shape. Thus, active nematic order of cells controls the stress fields required to shape bulky tissues. Recent theoretical considerations have suggested that the introduction of a curved field can control the onset of spontaneous tissue flow and a wide variety of flow structures, depending on the magnitude and the sign of curvature[66].

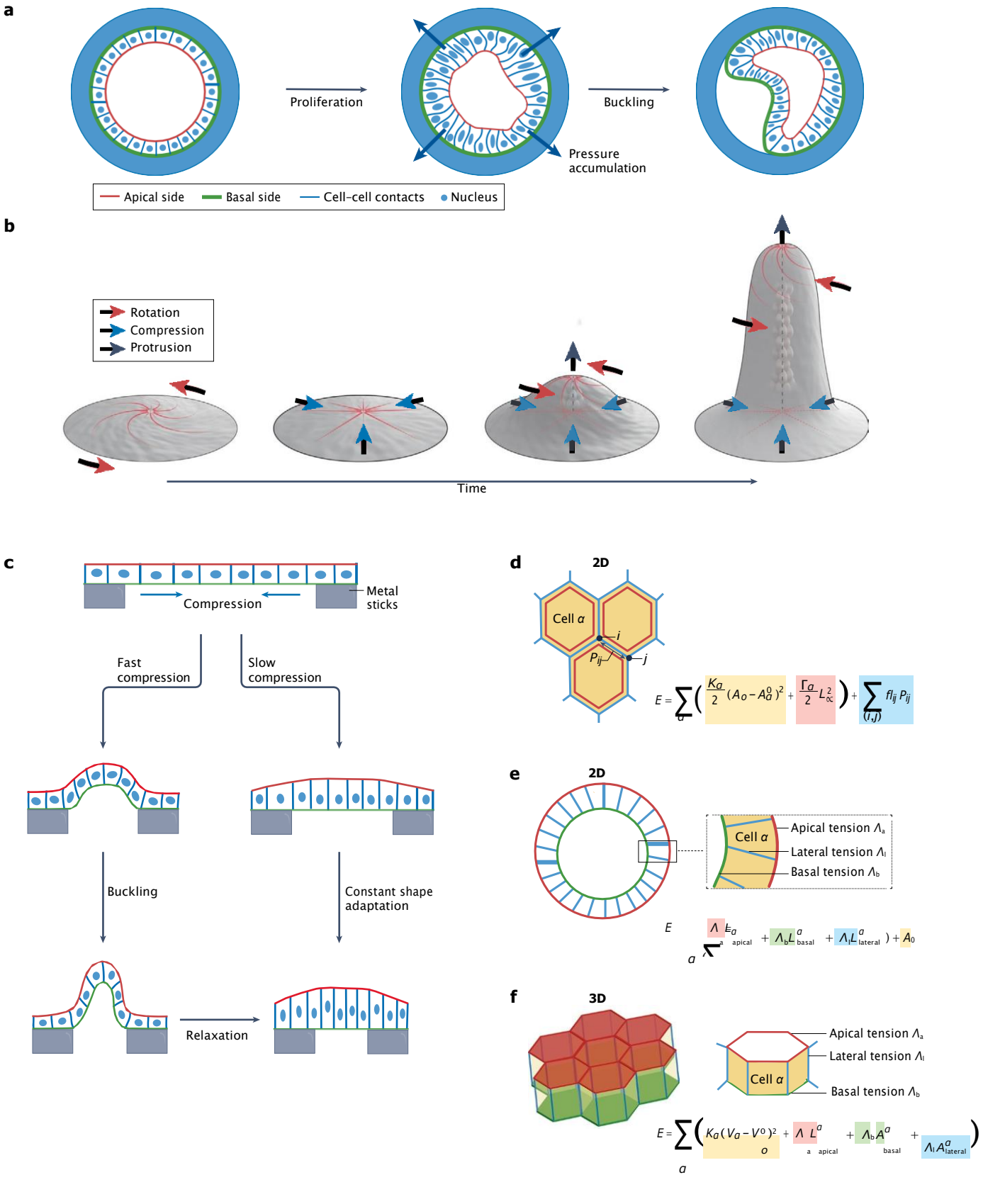
a
Proliferation
Buckling
Pressure accumulation
Apical side
Basal side
Cell–cell contacts
Nucleus
b
Rotation
Compression
Protrusion
Time
c
Compression
Metal sticks
Fast compression
Slow compression
Buckling
Constant shape adaptation
Relaxation
d
2D
Cell α
i
j
P_{ij}
$E = \sum_{\alpha} \left(\frac{K_\alpha}{2}(A_\alpha - A_\alpha^0)^2 + \frac{\Gamma_\alpha}{2} L_\alpha^2 \right) + \sum_{(i,j)} f l_{ij} P_{ij}$
e
2D
Cell α
Apical tension Λ_a
Lateral tension Λ_l
Basal tension Λ_b
$E = \sum_{\alpha} \left(\Lambda_a L^{\alpha}_{\text{apical}} + \Lambda_b L^{\alpha}_{\text{basal}} + \Lambda_l L^{\alpha}_{\text{lateral}} \right) + A_0$
f
3D
Cell α
Apical tension Λ_a
Lateral tension Λ_l
Basal tension Λ_b
$E = \sum_{\alpha} \left(K_\alpha (V_\alpha - V^0)^2 + \Lambda_a L^{\alpha}_{\text{apical}} + \Lambda_b A^{\alpha}_{\text{basal}} + \Lambda_l A^{\alpha}_{\text{lateral}} \right)$

Fig. 2 | Mechanisms of tissue curvature generation and vertex models. **a**, An epithelium growing in an elastic hollow sphere (blue) accumulates pressure that makes it buckle[61]. **b**, Nematic order of muscle cells confined on a disc forms a spiral that transitions into an aster, which further grows into a vortex, resulting in protrusion through proliferation[65]. **c**, A suspended epithelial monolayer under compression deforms in two different ways depending on the speed of compression. Under fast compression, the epithelium buckles and then flattens through cellular shape change. Under slow compression, the cells adapt their shape to accommodate the deformation, whereas the epithelium stays flat. **d**, The vertex model was developed to describe the paving shapes of cells in a flat epithelium[89]. Each cell has an elastic energy (K) around a preferred area (A^0) (yellow), a line tension energy term (Λ) corresponding to cell–cell adhesion (blue) and membrane tension and a contractility term (in red) which has the form of a linear elasticity term. The two vertices (black dots) are labelled with indices i and j. The connecting junction length is denoted by L_{ij} and the coefficients K_a, Λ_{ij} and Γ_a correspond to the area cell elasticity of cell a, the line tension of junction (i,j) and perimeter contractility of cell a, respectively. **e**, Vertex model that distinguishes three types of sides (apical, basal and lateral), all of which are line tension energies (Λ) with associated length (L) in this description[90]. The area of cells (A) is a fixed value and cannot change. **f**, The 3D vertex model is composed of the three surface tension energy terms corresponding to the three types of sides (apical, basal and lateral). Cell–substrate energy term proportional to the basal area (A_{basal}). Cell–cell lateral energy term proportional to the lateral area (A_{lateral}) and an energy term associated to the tension of the apical contractile part proportional to the apical perimeter (L_{apical}). The first term is an elastic volume energy term (yellow). Part **a** adapted with permission from ref. 61, Elsevier. Part **b** reprinted from ref. 65, Springer Nature Limited.

Impact of curvature induction on cell forces

Apart from cellular forces contributing to tissue curvature formation, in many instances, tissue curvature results from forces exerted by adjacent tissues. In such cases, cells within the bending tissue adjust to the altered curvature. To understand this adaptive process, suspended epithelial layers were cultured between two metal sticks and rapidly subjected to buckling by bringing the sticks closer together[67] (Fig. 2c). Notably, the cellular response depends on the speed of stick convergence. When performed slowly, cells contract and reorganize, maintaining a columnar epithelium and preserving a consistently flat tissue. Conversely, if the sticks are rapidly brought together, the epithelium buckles initially and then relaxes through cell contraction, ultimately returning to the flat columnar state observed with slower convergence. The proximity of the sticks during this process is crucial: compression <30% of the initial length results in curved epithelia that remain buckled. This finding underscores that the primary response of epithelial cells to buckling is an active attempt to revert to a flat state, likely restoring the overall contractile stress field. This phenomenon bears resemblance to the flattening effect of apical tension observed on periodically curved substrates.

To investigate whether convex or concave curvature leads to distinctly different mechanical states over a short timescale, epithelial monolayers were subjected to dynamic deformations in either a convex (towards the apical side) or a concave (towards the basal side) direction using deformable microsystems[68]. In response, epithelial cells exhibit a rapid wave of intracellular calcium signalling or, depending on the folding orientation, changes in gene expression within a few hours. Calcium waves were exclusively observed at the epithelium–substrate boundary under concave deformation, in which tension and curvature were the most pronounced. Conversely, the impact on gene transcription was only noticeable when the convex curvature was applied, leading to a decrease in membrane tension. This finding highlights that curvature can elicit a specific genetic response over longer timescales by inducing signal transduction, probably dependent on mechano-sensitive calcium channels.

Very few experimental systems enabling dynamic modulation of tissue curvature have been employed thus far. A deeper understanding of the impact of convex or concave curvature on tissue relies on the ability to study both force and stress equilibriums within tissues at very short (<1 min) timescales, as well as the functional response of tissues. In this regard, a flat epithelium was grown on a pre-strained substrate, and rolled upon cutting the substrate, releasing the strain[69]. The main change observed is cell swelling: in the roll, cells transiently increase their volume by ~50% 5 min after rolling and recover completely within 30 min. Interestingly, the effect is observed regardless of the sign of curvature, but if cells are periodically curved, inducing periodic hills and valleys, the volume does not change. The swelling is correlated with a complete depolymerization of the apical actin belt, and a decrease of membrane tension, again showing how all subcellular forces are coupled. The primary effect of this depolymerization is probably to decrease membrane tension, which the cell probably perceives as an osmotic shock, inducing swelling to restore tension. As a matter of fact, inhibition of the main ionic transporters involved in the osmotic balance of the cell affected the swelling and its recovery.

In future investigations, the application of Förster resonance energy transfer (FRET) tension sensors holds promise for revealing the dynamics of force transmission at focal adhesions and cell–cell contacts in response to dynamic curvature changes[70]. FRET sensors use an elongation-reporter system, consisting of two fluorophores — an energy donor and an acceptor — with distinct yet overlapping excitation and emission spectra. The FRET sensor can be considered as a molecular spring between the two fluorophores with a rate of energy transfer (K_{FRET}) as:

$$K_{\text{FRET}} \sim \frac{\kappa^2 J k_f}{n^4 r^6},$$

in which κ is the relative dipolar orientation between the donor and the acceptor, J is the integral of the overlap between the donor-emission and the acceptor-excitation spectra, k_f is the radiative emission rate of the donor, n is the refraction index of the medium and r is the distance between the donor and the acceptor[71]. Implementing these FRET tension sensors would provide valuable insights into the mechanical forces involved in cellular responses to varying curvatures. However, the tensional state of a specific protein as reflected by FRET sensors does not reflect exactly the stress in the epithelial monolayer. The internal stress distribution in the tissue can be obtained using the monolayer stress microscopy (MSM) technique[72]. In this technique, the monolayer is modelled as a very flat plate under plane-stress conditions and the equilibrium is described as

$$\frac{\partial \sigma_{xx}}{\partial x} + \frac{\partial \sigma_{xy}}{\partial x} = \frac{T_x}{h}$$

$$\frac{\partial \sigma_{xy}}{\partial x} + \frac{\partial \sigma_{yy}}{\partial x} = \frac{T_y}{h},$$

in which σ_{xx}, σ_{yy} and σ_{xy} are the components of the stress tensor in the tissue, h is the mean height of the monolayer and T_x and T_y are the tractions

measured by traction force microscopy. However, these two partial differential equations alone do not provide enough information to determine the three unknown stress components. They need to be supplemented by the Beltrami–Michell compatibility condition[73–75]:

$$\frac{\partial^2}{\partial x^2} + \frac{\partial^2}{\partial y^2}(\sigma_{xx} + \sigma_{yy}) = \frac{1+\nu}{h}\left(\frac{\partial T_x}{\partial x} + \frac{\partial T_y}{\partial y}\right),$$

in which ν is the Poisson's ratio of the monolayer. An implicit assumption in this equation is that the tissue exhibits linearly elastic isotropic behaviour. The inferred MSM tissue stress is subsequently derived by solving these equations with appropriate boundary conditions. The MSM method has been adapted to curved epithelial monolayers to map their tensional stress[76]. Interestingly, a weak, size-independent increase in stress with areal strain was observed in spherical geometry, whereas epithelia with rectangular and ellipsoidal cross-sections were characterized by distinct stress anisotropies influencing cell alignment.

A model system to quantitatively assess the tissue force balance

Epithelia are single-cell monolayers that separate tissues or cavities from their environment. The skin, intestinal and lung surfaces are classic epithelia. These epithelia typically possess a thickness ranging from a few to a few tens of micrometres and exhibit apico-basal polarity. The basal surface is defined by cell-substrate adhesions, whereas the apical surface is exposed to the environment and houses a contractile actomyosin belt. Epithelia are thus considered as bidimensional tissues, with a prototypical hexagonal cell shape, and a simple architecture of force-generating components. These features make the epithelium a model of choice to understand how subcellular forces can be integrated to generate large-scale forces in relation with the shape of cells.

Tissue architecture and cell shape. Epithelial cells on a flat substrate have a 3D shape that can be modelled as contiguous hexagonal prisms of base length r and height h. Epithelial cell shapes are classified depending on their aspect ratio: columnar (tall and thin, $h/r \gg 1$), squamous (flat and spread out, $h/r \ll 1$) and an intermediate cuboidal shape ($h/r \approx 1$). To accommodate curvature, cells can adopt conical or inverted conical shapes, wherein the disparity in area between the apical and basal sides corresponds to the discrepancy imposed by the curvature. These simple shapes perfectly adapt cell shapes to isotropic curvature (sphere and dome).

In more complex structures, in which curvature is anisotropic (cylinders and ellipsoids) or changes sign (branched network), the shape can be a scutoid[77,78]. Scutoids are geometrical shapes in which the number of neighbouring cells on the apical side differs from that on the basal side[79]. In these cells, there is a change of contact cells along the z axis, like in the apico-basal T1 (AB-T1) transition. Although these shapes are not at energy minimum per se, they tend to minimize the overall energy cost associated with the area change from apical to basal in highly anisotropic curved surfaces. This is supported by the fact that scutoids are found in dry foams confined between curved surfaces, and predicted from simulations based on surface energy minimization[80], also suggesting that scutoids are stable in time[77].

Tissue curvature plays a pivotal role in AB-T1 transitions, particularly in regions characterized by low curvature anisotropy, such as the *Drosophila* embryo head[81]. Within 3D environments featuring a pronounced curvature gradient, cells exhibit a tilting behaviour to optimize packing efficiency. The resulting tilted lateral membranes generate tensions, contributing to in-plane stresses with opposite signs on the apical and basal planes, consequently initiating AB-T1 transitions. Lateral membranes crucially modulate stress distribution within cells, influencing cell shape regulation[82]. Reduced contractility in lateral membranes induces cell tilting, interacting with pressure and tissue thickness to yield a diverse phase diagram for AB-T1 transitions. Increased stiffness in lateral membranes suppresses tilting, causing AB-T1 transitions in regions with significant curvature anisotropy, aligning with hydrostatic limit predictions.

Vertex models. Epithelial tissues are out-of-equilibrium, but can be described in a first approximation using a mechanical equilibrium as the minimization of an effective energy, E. The primary components of E include the energy of cell-substrate adhesion, the energy of intercellular adhesion, the energy associated with volume control and the energy provided from the tension exerted by the apical actomyosin belt[83,84]. However, these ingredients must be combined with geometrical constraints of cells and tissue shape to reliably describe the mechanical state of the epithelium. Attempts to have a mechanical model that reproduced shapes of both cells and tissues date to 1902, when an assembly of elastic cells made of corset bones of different lengths, lacing and wires to apply forces was used to reproduce observations of gastrulation in sea anemones[48].

Mathematical models of epithelia make it possible to anticipate shapes based on the mechanical characteristics of tissues and cells[85,86]. The goal is to describe shapes of cells during gastrulation of simple organisms using a 2D circle of cells. The main limitation of early models is that they do not separate well from the different types of forces (adhesion, osmotic pressure and contractility). Later, force terms related to geometrical changes were introduced[87]. Area and perimeter length changes are used to calculate three tension terms, the area, the edge and the angular tensions. Such formalization of different forces was reused in a dynamic, out-of-equilibrium computation of different tessellations of epithelial cells from their force distribution[88].

Refined 2D vertex models were introduced to better predict the tessellation of epithelial cells from cellular forces by proposing a more accurate force balance equation[89] (Fig. 2d). In this case, the force balance at each vertex combines a tension term corresponding to membrane tension, a surface elastic term for the apical area corresponding to osmotic pressure and an elastic term along the perimeter corresponding to the actin contractile ring force. Energy minimization of the global force balance, using cells with the same resting area and perimeter length, predicts well the distribution of neighbours and the shapes of cells. Vertex models can adapt to any epithelium geometry and identify the specific contributions of each vertex. Apart from describing the tessellation of epithelial cells, vertex models predict gastrulation shapes with or without the need for apical constriction[90] (Fig. 2e). The energy of the system arises from the three types of cell sides — lateral (Λ_l), basal (Λ_b) and apical (Λ_a) — the line tensions of which can be modified independently. In this case, the area of surface is considered constant.

Expansions of vertex models to 3D have predicted buckling of epithelia[83] and the contribution of baso-lateral tensions in tissue deformation[91] (Fig. 2f). A limitation of vertex models is the number of parameters used, which allows fitting the models to any experimental observation, but with low reliability on the parameter values. Moreover, changing tension terms (constant force with extension) to spring terms (force proportional to extension) usually changes the parameter values, but not really the predictions.

Mechanisms of cellular and nuclear curvosensing

In-plane curvature

Single-cell level. Surface micropatterning is a powerful technique for studying the effect of 2D geometrical cues on individual cells[92–94] or small cell assemblies by imposing adhesive patterns and chemical boundaries. On 2D surfaces, focal adhesions occur most prominently along adhesive zones, and stress fibres along non-adhesive zones. On protein micropatterns with shapes such as crossbow or square, lamellipodial extensions were preferentially formed at the convex zones (Fig. 3Aa) owing to accumulated tractional forces and the concentration

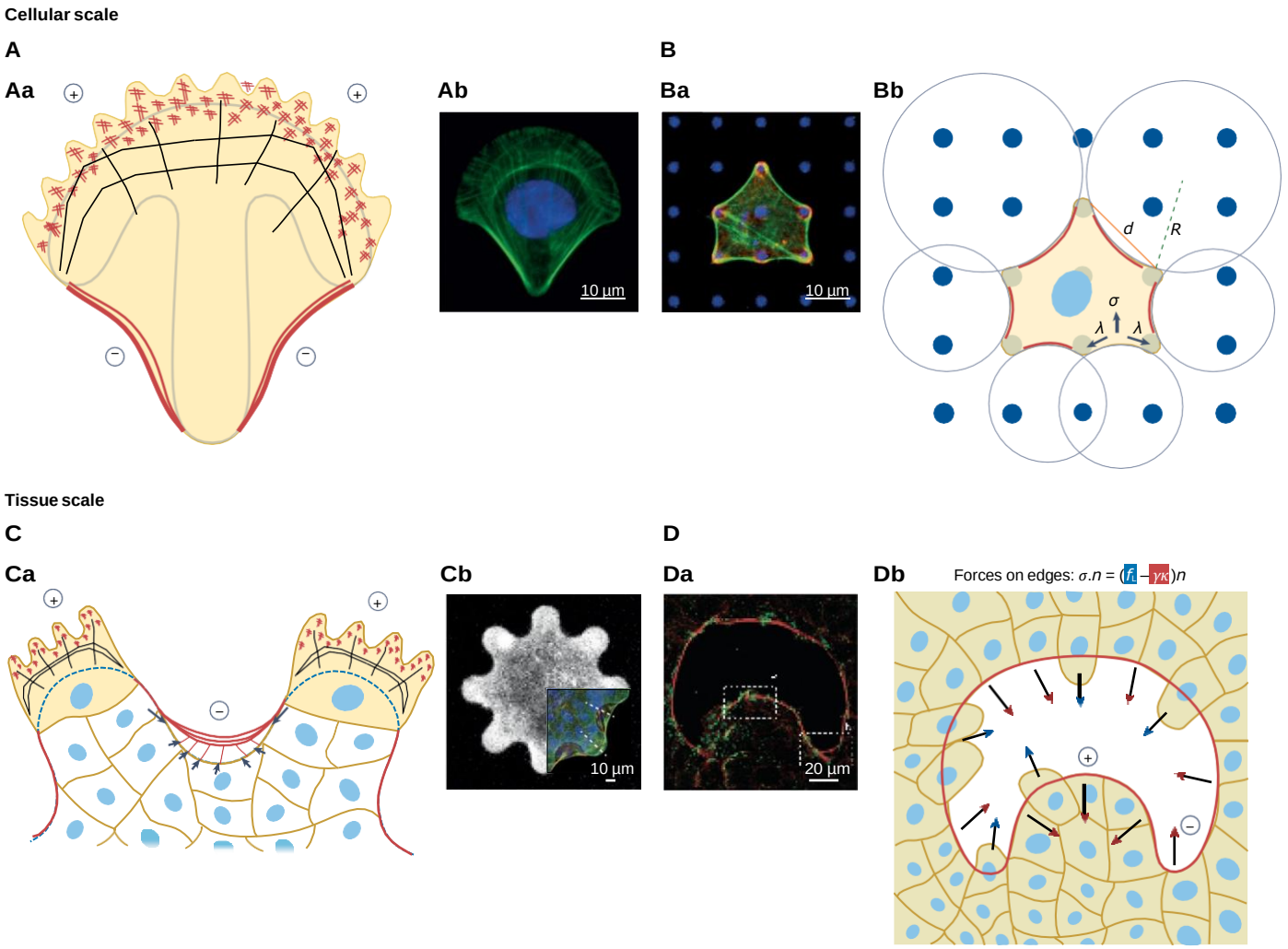

Fig. 3 | In-plane curvature at cellular and tissue scales. Aa, Actin cytoskeletal architecture in a single epithelial cell plated on a crossbow-shaped micropattern with a branched actin network in the lamellipodia (positive curved edge) and actin stress fibres above non-adhesive zones (negative curved edges). **Ab**, Fluorescent image of the spatial organization of the actin cytoskeleton (green) in an epithelial cell plated on an adhesive crossbow-shaped micropattern. Stereotypical actin architecture, featuring a branched network in the lamellipodium along the curved adhesive edge. This network reorganized in the lamella, forming radial fibres perpendicular to the curved edge and transverse arcs along the same edge. Additionally, a pattern of ventral stress fibres emerged above non-adhesive edges, flanking the central bar in a crossbow configuration. The nucleus (blue) is located at the centre of mass of the cell. **Ba**, Single cell cultured on micropatterned dots (blue) showing circles that fit well with arc-like contours of the cells. For each arc, the radius R and the spanning distance d are measured. The line tension λ acts to straighten the contour between adjacent adhesions, and the surface tension σ pulls the envelope inward towards the bulk. In mechanical equilibrium, R is locally determined by λ/σ and remains independent of d. **Bb**, Fluorescent image of cell shape on micropatterned fibronectin dots showing an arc-like contour composed of actin fibres (green) and paxillin (red). **Ca**, Epithelial cells on a part of a flower-micropatterned surface showing lamellipodia formation at positive curvatures and suspended cell parts over non-adherent areas at negative curvatures. A supracellular actomyosin cable exerts high contractile forces in the negatively curved region of the pattern. **Cb**, Image of a micropatterned tissue of epithelial cells. Phalloidin is labelled in red, myosin IIA in green, nucleus in blue and fibronectin pattern in cyan. **Da**, Gap closure with a combination of contractile cables and cell crawling. Local curvatures of the epithelium edge induces either lamellipodia extension (purple arrow) or actomyosin cable assembly (red arrow). Contribution of two forces: crawling forces owing to lamellipodium extension, F_L, and purse-string forces, $\gamma\kappa$, in which γ is the line tension and κ is the local curvature ($=1/R$). **Db**, Immunofluorescence staining of actin (red) and paxillin (green) of the gap at different curvatures (N, negative; P, positive). Part **Ab** reprinted with permission from ref. 97, Company of biologists. Parts **Ba** and **Bb** adapted with permission from ref. 100, Elsevier. Parts **Ca** and **Cb** adapted from ref. 107, Springer Nature Limited. Part **Da** is adapted from ref. 110, CC BY 4.0. Part **Db** is reprinted from ref. 110, CC BY 4.0.

of mature focal adhesion sites[94–97]. Branched actin network forms in the lamellipodia at the positive curved edge, whereas actin stress fibres are located at negative curved edges, above non-adhesive zones (Fig. 3Ab). In addition, high aspect ratios and subcellular curvatures enhanced the cellular contractility and led to osteogenic differentiation[98], whereas rounded cell morphologies promoted adipogenesis[99].

The interaction among local curvature, cytoskeletal anisotropy and the geometric constraints imposed by the spatial distribution of focal adhesions was investigated with micropatterned cells by approximating the cell edge with a series of circular arcs (Fig. 3B). The spatial distribution of focal adhesions can dynamically adapt to different geometrical constraints, resulting in the formation of curved edges in individual cells, akin to a tent canvas stretched between its pegs. The reason for the formation of these curved edges lies in the high tension between focal adhesion points. The eccentricity of the arcs depends on the level of anisotropy in the contractile stresses generated by the contractile actomyosin network[100] (Fig. 3Ba). Consequently, the cell shape can be described based on a geometry-dependent distribution of a surface tension, with contractile forces retracting the cell inwards towards their centre of mass. Intuitively, contractile forces work to reduce the surface area of the cell, whereas opposing forces, such as line tension, arise from the resistance of the cell boundary to length extension. Surface tension and line tension maintain a local equilibrium along the contour of the cell, counterbalancing each other (Fig. 3Ba), and the degree of anisotropy in contractile actomyosin fibres regulates the eccentricity of the circular arcs. The cell contour evolves subject to a competition between internal and external bulk stresses acting on the cell boundary and the tension arising within the cell cortex. At the cellular level, a feedback mechanism regulates the alignment of stress fibres parallel to the cell edge and uniformly across the entire cell[101]. Collectively, these findings demonstrate that dynamic cell contour changes are controlled by the interplay between the stresses exerted on the cell boundary and the tension within the cell cortex. This interplay allows for the prediction of both cellular morphology and the spatial distribution of stress fibres.

Protein micropatterns were used to investigate the influence of cell-size positive and negative curvatures on the polarization of metastatic cells[102]. Cells adhering to these surfaces respond to local curvature at the perimeter of the adhesive islands. Stress fibres were mostly present across non-adhesive space of concave edge and lamellipodia-like structures were formed at the region with high convexity[102]. Furthermore, it was established that polarity in tumour cells is sensitive to both the global aspect ratio of the pattern shape and the local curvature of adhesive micropatterns[94,102] and that the alignment of stress fibres exhibits a strong correlation with the direction of cell polarization[103–106].

Collective cell level. Similar findings were observed in epithelial tissues cultured on adhesive micropatterns with flower-like shapes, which contain both convex and concave domains. Cells form protrusions at positive curvature zones[107], whereas a supracellular actomyosin cable exerts high contractile forces in the negatively curved region of the pattern (Fig. 3C). Gap closure experiments involving both convex and concave features demonstrated the impact of in-plane curvature on the two distinct mechanisms involved in wound closure: cell crawling[108] and purse-string contractions[109,110] (Fig. 3D). Negative curvatures stabilize the formation of robust contractile actin cables, whereas positive curvatures promote the assembly of persistent lamellipodial extensions, with a perturbation actomyosin cable continuity (Fig. 3Da). At the edge of the gap, crawling forces exerted perpendicular to the edge drive cells forward, resulting in nearly constant edge speeds across all curvatures. However, these crawling forces are counteracted by purse-string forces ($\gamma\kappa$), in which κ represents the local curvature and γ is the tension exerted by the actomyosin cable, which pulls the edge backward in positive regions and forward in negative regions (Fig. 3Da). In positive curvature zones, purse-string contraction positively pairs with cell crawling in negative curvature zones, resulting in higher velocities.

On substrates with heterogeneous curvature, cell shape changes give rise to distinct arrangements of the actin cytoskeleton, resulting in functional modifications such as the formation of contractile actomyosin cables and lamellipodial protrusions[110]. In addition to in-plane curvature changes, cells also interact with the curved topography of their microenvironment (curvotaxis). The curvature occurs across several length scales. Two questions arise: how can topographical features modulate cell-level and tissue-level functions, and to which curvature length scale (from nanometre to micrometre) are adherent cells sensitive? Addressing these questions is crucial for understanding fundamental physiological processes and can provide insight for the design of new therapeutic devices.

Out-of-plane curvature

Nanometre scale. The nanoscale characteristics of the ECM influence diverse biological processes, and the lateral nanospacing of integrins plays a role in governing single-cell functions such as spreading and migration[111–113]. Additionally, lateral adhesion spacing regulates intracellular force generation, consistent with the molecular clutch model[114]. Exploring the intricate interplay among cell adhesion, the cytoskeleton and surface nanoengineering techniques can provide insights into how cells perceive their nanoenvironment and respond to curvature changes at the nanoscale. Interactions between human bone osteosarcoma epithelial cells and nanopillars of radii of 100–1,000 nm revealed actin accumulation on the curved lateral surface of the pillars, rather than on the flat areas of the substrate[115] (Fig. 4a). Actin accumulation was more pronounced on smaller nanopillars, suggesting a curvature-dependent formation of actin fibres with an upper curvature limit at around 400 nm (ref. 18). This finding was confirmed using nanobars with long straight sides and curved ends, in which actin fibres accumulated at the curved extremities, mediated by a multiprotein (Arp2/3) complex (Fig. 4a), which is a key regulator of actin polymerization, and curvature-sensing proteins of the BAR-domain protein family. The formation of actin fibres in response to nanotopographical features led to a notable reduction in mature focal adhesions and results in a profound remodelling of the entire actin network.

Under physiological conditions, cells encounter more complex curved nanostructures, such as ECM fibres. Cells first extend numerous lamellipodial extensions to explore their microenvironment composed of a meshwork of fibres and then establish a stable cellular protrusion, which defines the front-rear axis[116]. The diameter of the fibre influences the spatial distribution of focal adhesions[117], which play a role in generating traction forces. Interestingly, normal epithelial cells developed shorter protrusions than did highly metastatic breast adenocarcinoma cells when encountering suspended fibres of different diameters[118]. These results suggest that metastatic cells exhibit better adaptability to the nanoscale curvature of the fibrous collagen matrix. In vitro investigations revealed that metastatic breast cancer cells possess the ability to sense fibre curvature by wrapping around them, exhibiting a coiling rate that increases in a curvature-dependent fashion[119] (Fig. 4b). There are also reports of curved adhesions that mediate the 3D cellular

attachment to nanometric fibres and are involved in the migration of tumoural cells[120]. The dimensions of the ECM fibres imposed specific membrane curvatures that in turn are regulated by the formation of curved adhesions.

Micrometre scale. At a larger scale, cells encounter surfaces with radii of curvature spanning the range of cell sizes (~20–100 µm), which are prevalent in numerous biological systems. The significance of micrometre-scale curvature was explored in the 1940s when Schwann cells were cultured on glass fibres with radii of 13 µm, revealing cell alignment along the axis of the cylinders[121]. Subsequently, it was proposed that the extent of axial alignment inversely correlates with the cylinder radius, emphasizing the importance of micrometre-scale curvature as a crucial ECM cue capable of modulating cell locomotion via modifications of the cytoskeleton[122]. Intriguingly, although numerous cell types align along the axial direction on cylinders with radii equal to their length scale, most cell types do not adopt preferential alignment on larger cylinders[123]. The current hypothesis considers that cell alignment on small cylinders allows avoiding the energy penalty required to bend along stress fibres.

Despite considerable progress in investigating cellular responses to curvature, experiments perturbing the activation of Rho, which governs the assembly of contractile fibres, have reported counter-intuitive observations[123]. Surprisingly, the alignment of thick stress fibres in the circumferential direction of low-curvature cylinders was observed when Rho was activated, defying the expectation that thicker stress fibres would exhibit enhanced axial alignment owing to their increased resistance to bending. Moreover, certain cell types exhibit a distinct lack of curvature response, characterized by a small population of short stress fibres wrapping around the circumference, indicating substantial bending. This phenomenon is reminiscent of in vivo scenarios encountered by pericytes, smooth muscle cells and endothelial cells, in which complex curvatures are shaped by tubular blood vessels[124]. For instance, pericytes encircle small capillaries with extensions in a circumferential manner[125], whereas vascular smooth muscle cells were oriented in the circumferential direction or adopted helical patterns within cylindrical tissues[126]. Moreover, the sign of curvature should also be considered in determining the mechanism of cell adaptation to curvature. For example, as the curvature increases on convex channels, renal epithelial cells align their in-plane axis perpendicular to the channel without changing their morphology, whereas on concave channels, renal cells elongate and exhibit longitudinal directionality[127].

Thus, although the concept of actin bending penalties remains important in understanding curvature cues, relying solely on bending energy arguments is not sufficient to explain the different cell orientations or the organization of actin filaments. Additional mechanisms, such as actomyosin contractility, may be at play[128]. To gain further insights into the mechanical adaptation of cytoskeletal force balance in response to complex out-of-plane curvature patterns, fibroblasts were cultured on axisymmetric sphere-with-skirt substrates[129] (Fig. 4c). These substrates consist of convex caps (positive curvature) transitioning smoothly towards flat surroundings through a saddle-shaped region (negative curvature). Although most cells avoid the cap part, occasional probing occurs using short-lived lamellipodia. Two distinct subpopulations of stress fibres were observed in fibroblasts on the skirt region: apical stress fibres (above the nucleus), aligning radially to avoid bending, and basal stress fibres (below the nucleus), aligning circumferentially (Fig. 4c). Interestingly, the apical stress fibres do not conform to the local concave curvature of the substrate but bridge this concavity instead.

In addition to single-cell studies, additional research has explored the role of matrix curvature in confluent monolayers. When plated at confluency, fibroblasts undergo elongation and alignment with neighbouring cells, leading to the formation of co-alignment domains of ~500 µm in size. This process also gives rise to the formation of topological defects[130,131]. These observations have led to the introduction of an additional physical cue based on the nematic order, as observed in liquid crystals, to understand fibroblast behaviour in confluent monolayers. Nonetheless, when cells are cultured on cylindrical substrates, their alignment patterns deviate from the anticipated helical wrapping patterns predicted by the nematic theory. Contrary to expectations, cells within confluent monolayers exhibit strong axial alignment cylinders with low curvatures[123], suggesting that the underlying mechanisms governing the alignment of cells in curved monolayers are more complex than alignment phenomena in active nematics.

More recent studies have used wavy substrates to investigate the individual roles of concave and convex curvatures on confluent epithelial monolayers[84,132,133]. These monolayers do not form nematic orders but exhibit a highly ordered distribution of packed polygonal cells. Although micrometre-scale curvatures do not affect the organizational rules in epithelia, epithelial cells are thicker in concave valleys compared with when they are negatively curved on convex crests, leading to local variations in monolayer thickness on corrugated substrates[84] (Fig. 4d). These observations were described using vertex models based on the assumption that the morphology of epithelial cells is primarily determined by the balance between tension generated by the actomyosin cortex, cell–substrate adhesion and cell–cell adhesion[134]. Finally, at curvature length scales much larger than the cell size, cell guidance is dominated by nanoscale contact guidance along collagen fibrils.

A better understanding of the physical mechanisms that underlie cellular responses to mesoscale curvatures would not only provide insights into the regulation of cellular tension by curvatures at various length scales but also how various mechanotransduction pathways synergistically determine downstream cellular functions. In addition to this challenge, additional studies should also investigate the impact of curvature length scale on cell migration on curved substrates.

Curvotaxis and cell migration on curved substrates

Cell migration involves intricate interactions between the cell–substrate interface, cell polarization and propulsive forces. The migratory capacity of cells is crucial for numerous physiological functions and is also implicated in tissue morphogenesis during developmental processes. Importantly, cell migration drives pathological conditions that include cancer invasion and metastasis. Extensive research has focused on studying how physicochemical parameters of the cell microenvironment, such as rigidity, viscoelasticity and cell–ligand density, influence cell migration. Emerging evidence suggests that local changes in curvature of the cell microenvironment can also influence cell migration, notably by modulating cytoskeletal arrangements within membrane protrusions, such as filopodia and lamellipodia, which are key drivers of cell movement. However, the precise mechanisms by which the length scale of curvature in the ECM regulates cell migration at single and collective levels remain poorly understood.

Single-cell migration. To investigate how single cells adapt their locomotion to the curvature imposed by ECM fibres, such as collagen and elastin of a few hundred nanometres in diameter, in vitro experiments

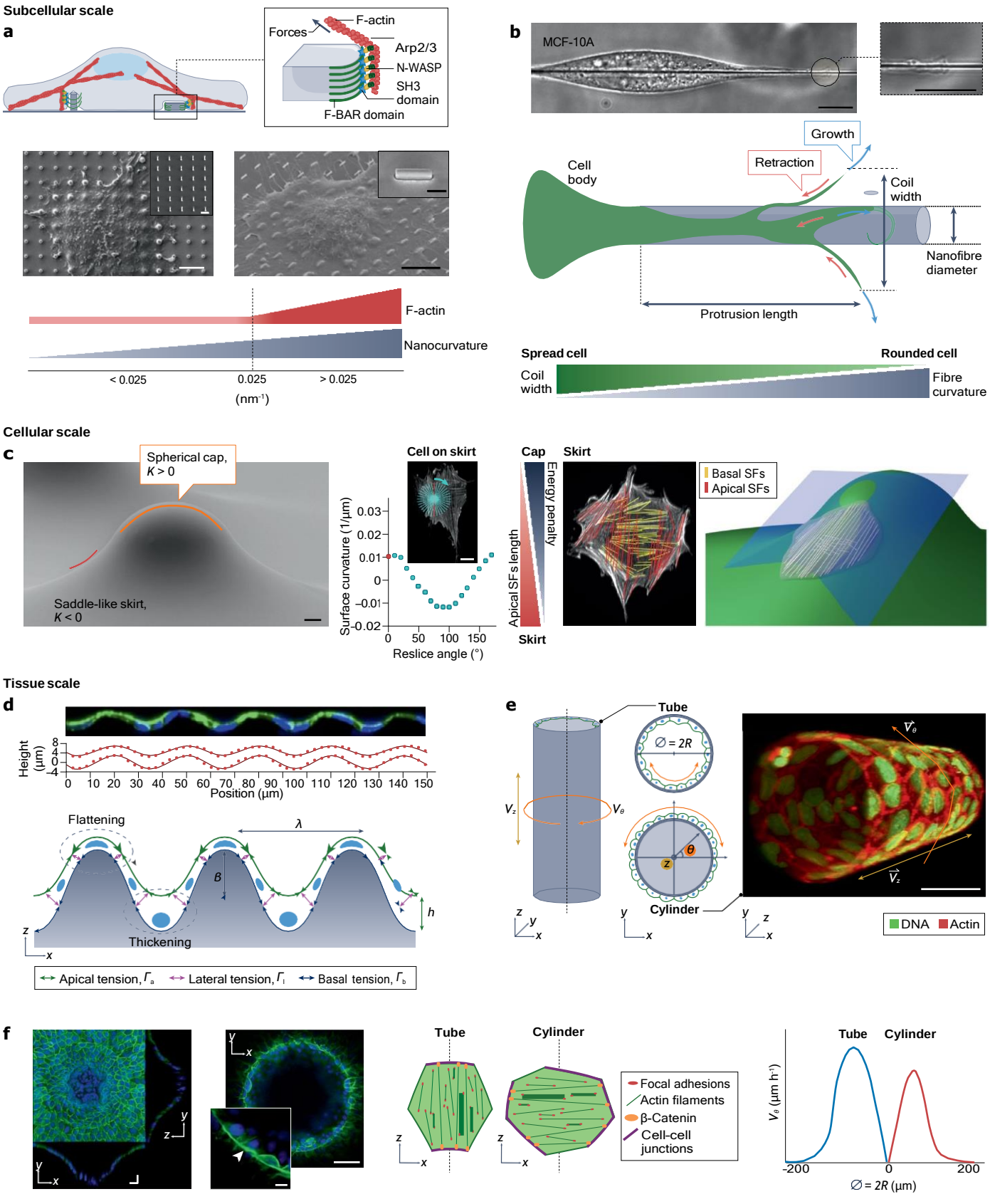
Subcellular scale
a
Forces
F-actin
Arp2/3
N-WASP
SH3 domain
F-BAR domain
F-actin
Nanocurvature
< 0.025
0.025
> 0.025
(nm⁻¹)
b
MCF-10A
Growth
Retraction
Cell body
Coil width
Nanofibre diameter
Protrusion length
Spread cell
Rounded cell
Coil width
Fibre curvature
Cellular scale
c
Spherical cap, K > 0
Saddle-like skirt, K < 0
Cell on skirt
Surface curvature (1/μm)
0.03
0.02
0.01
0
−0.01
−0.02
0
50
100
150
Reslice angle (°)
Cap
Skirt
Energy penalty
Apical SFs length
Skirt
Basal SFs
Apical SFs
Tissue scale
d
Height (μm)
8
4
0
−4
0 10 20 30 40 50 60 70 80 90 100 110 120 130 140 150
Position (μm)
Flattening
λ
β
h
Thickening
z
x
Apical tension, Γa
Lateral tension, Γl
Basal tension, Γb
e
Tube
∅ = 2R
Vz
Vθ
θ
z
Cylinder
DNA
Actin
f
y
z
x
Tube
Cylinder
Focal adhesions
Actin filaments
β-Catenin
Cell-cell junctions
Tube
Cylinder
Vθ (μm h⁻¹)
-200
0
200
∅ = 2R (μm)

Fig. 4 | Multiscale out-of-plane curvatures. a, Curvature-dependent formation of actin filaments around nanobars. The curvature is recognized by F-BAR domains, and SH3 domain of FB1 7 interacts with N-WASP to promote Arp2/3-initiated F-actin polymerization. Scanning electron microscopic image of vertical nanopillar with tubular (left) and nanobar (right) geometries. The sketch shows the threshold of nanocurvature leading to F-actin formation. **b**, Representative image of coiling by an epithelial cell (MCF-10A) along a nanometric fibre. Scale bar, 10 μm. Schematic representation of the coiling dynamics with retraction and growth movements. The sketch shows the inverse relationship between the coil width and the fibre curvature. **c**, Left to right: scanning electron microscopic image of a sphere-with-skirt surface, with a scale bar of 50 μm. The curve illustrates the variation of the local curvature field around each stress fibre obtained from radial reslice lines (cyan dots) around a reference stress fibre (red dot). The sketch illustrates the inverse relationship between the energy penalty owing to bending (in grey) and the length of apical stress fibres (in red). Projections of phalloidin signals (in grey) in cells on a skirt region are depicted, with red and yellow lines indicating apical and basal stress fibres, respectively. A schematic representation of the actin cytoskeleton of a cell on a sphere-with-skirt surface demonstrates the perpendicular alignment of stress fibre subpopulations. **d**, From top to bottom: representative confocal profiles (*xz*) and average thickness modulation for a corrugated hydrogel of 30 μm wavelength. Schematic of an epithelial monolayer grown on a corrugated hydrogel of amplitude β and wavelength λ. The balance between apical tension, lateral tension and basal tension leads to thickness modulation of the epithelial monolayer, with a flattening on the crest and a thickening in the valley. **e**, From top to bottom: a confluent Madin-Darby canine kidney monolayer (green) inside a tube with collective movements with longitudinal (V_z) and azimuthal (V_θ) velocities. Cross-sectional views of a cell monolayer that lays on either the inner (tube, in blue) or the outer side (cylinder, in orange) of a cylindrical substrate (dark grey) with associated azimuthal (V_θ, in orange) velocities. Representative 3D reconstructed images of a Madin-Darby canine kidney monolayer grown inside a tube of 100 μm diameter. White arrows show either V_θ or V_z. Schematic representation of the orientation of actin filaments and cell-cell junctions and the distribution of focal adhesions and β-catenin for tubular and cylindrical geometries. Representative V_θ as a function of the diameter of a tube (blue) and a cylinder (red). **f**, Typical confocal images showing top (*xy*) and side (*xz*; *yz*) views of a 3D microwell of radius 100 ± 3 μm covered by a confluent epithelial monolayer. The inset on the right shows a supracellular actin ring formed at the edge of a microwell of radius 100 μm. F-actin is in green and DNA in blue. Scale bars, 20 μm (left) and 50 μm (right). Part **a** reprinted with permission from ref. 187, PNAS. Part **b** adapted with permission from ref. 119, Elsevier. Part **c** adapted with permission from ref. 129, Elsevier. Part **d** adapted from ref. 84, Springer Nature Limited. Part **e** adapted with permission from ref. 156, AAAS. Part **f** reprinted with permission from ref. 158, Wiley. SFs, stress fibres.

were conducted using synthetic microfibres and nanofibres formed by phase separation[135] or electrospinning[136]. Although nanofibre curvature has a limited impact on cell migration persistence, it increased the cell migration speed by approximately a factor of 2.5 (ref. 137). Interestingly, the curvature that leads to the maximum migration speed was found to be cell-type-dependent, with 2.5 μm^{-1} for fibroblast mouse embryonic cells[137] and 5 μm^{-1} for mesenchymal stem cells (MSCs)[138]. Surprisingly, these maximum velocities decreased for larger and smaller fibre diameters, indicating a biphasic dependency of the cell velocity on curvature, as observed previously for other cues such as ligand density[139–141].

Various cell types exhibited substantial decreases in projected cell area and increased cell aspect ratios on small fibre diameters, suggesting cell elongation and reduced adhesion area[137,142,143]. Inhibition of Rho-associated kinases (ROCK) resulted in a decrease in migration velocity regardless of fibre curvature, and downregulation of the ROCK-1 gene expression was observed for larger fibre curvatures[144]. These findings collectively demonstrate that fibre curvature can modulate the cell migration velocity through the regulation of Rho/ROCK signalling, which is involved in the assembly of focal adhesions. Work is needed to confirm the existence of a curvature threshold and to explore the possible interplay between curvature and contact guidance.

At larger curvature scales (~10^{-2}–10^{-3} μm^{-1}), cells migrating on double sinusoidal surfaces tend to remain in concave regions (valleys) and avoid convex ones (crests)[145]. Individual human MSCs exhibit enhanced migration in concave tubular structures, whereas the expansion speed of epithelial tissues decreased notably in smaller tube diameters[146]. These observations could be explained by the fact that protrusive forces exerted towards the direction of migration are larger on concave surfaces than on convex ones[147], suggesting that the local curvature can direct cell motion during important biological processes[148].

Collective cell migration. Collective cell migration is influenced by substrate curvature across scales from nano to micro. Epithelial monolayers cultured on surfaces with a single principal curvature, such as convex cylindrical wires, expand along the tube axis, and the migration speed increases with the tube curvature[149]. Conversely, inside cylindrical pores, the migration speed of epithelial sheets decreases with increasing curvature[150,151]. On substrates that possess both concave and convex zones, the migration trajectories of epithelial tissues differ in each zone. Migration along high curvatures remains relatively straight, but the straightness of the migration front decreases as the substrate curvature decreases, indicating the formation of a migration front in the transverse direction[152]. The sensitivity to the curvature is cell-type-dependent. Osteoid-like tissues grown exclusively inside the concave areas of niches exhibit different growth rates on concave and convex spherical regions[153]. These findings were confirmed on more complex scaffolds with a constant mean curvature[154], suggesting that convex edges of substrates promote outward tissue extension, leading to effective flattening.

Although previous studies have focused on tubular systems for studying the expansion of epithelial monolayers on concave and convex substrates, only a few studies have looked at how curvature influences the dynamics of cell monolayers. Such studies show that epithelial cells can undergo global and persistent rotation on both concave and convex cylindrical substrates (Fig. 4e). Surprisingly, despite similar circumferential rotational dynamics, concave and convex surfaces exhibit distinct orientations of the contractile actomyosin network and opposite apicobasal polarities. Stress measurements conducted in flat epithelial monolayers revealed a phenomenon known as plithotaxis, wherein cells exhibit a preference for migration along the maximal principal stress component[155]. Experimental findings on curved substrates therefore challenge the conventional understanding that collective migration aligns with the principal stress component in 2D flat monolayers[156], and further investigation should study plithotaxis on curved substrates.

Unexpectedly, the Gaussian curvature of spheroids triggers an active velocity wave propagating along the spheroid equator, influencing collective cell migration[157]. The wavelength of this velocity

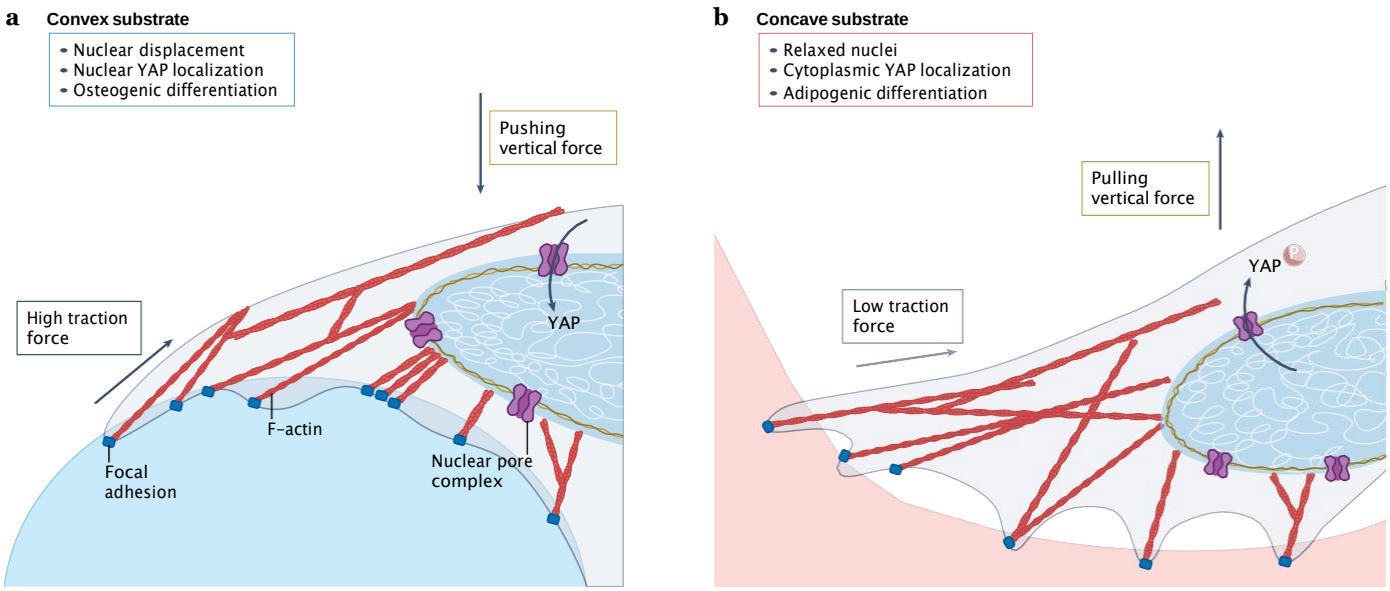

Fig. 5 | Nuclear curvosensing on concave and convex substrates. Geometry-induced changes in cellular attachment and forces on the nucleus for concave and convex surfaces. **a**, On convex surfaces, cytoskeletal forces exert a substantial push force towards the surface, causing compression and deformation of the nucleus. Mechanical forces on the nucleus promote osteogenic differentiation. Traction force measurements reveal stress gradients preceding and mirroring differentiation patterns, with high stress favouring osteogenesis on convex substrates and low stress promoting adipogenesis on concave substrates. This underscores the role of mechanical forces in shaping patterns of cell differentiation. **b**, On concave surfaces, cytoskeletal forces generate an upward pull force away from the substrate. The cell body is elevated, attaching only at distinct adhesion points, and the nucleus experiences a more relaxed state. The equilibrium between cell-inherent traction forces and geometry-induced pull forces reduces cytoskeletal and nuclear envelope tension, resulting in Yes-associated protein (YAP) cytoplasmic phosphorylation.

wave is found to be determined by the diameter of a spheroid, and the migration behaviour can be described using a theoretical model based on a monolayer of active particles constrained to a sphere. Interestingly, the straightness and speed of individual cells within a confluent epithelial tissue are enhanced at the concave entrance of 3D microwells that mimic lobular structures[158] (Fig. 4f). These modifications in collective migration are suggested to be related to the presence of a contractile supracellular actin cable promoted by the Gaussian curvature of the microwell. These findings illustrate how curvature and topology can shape collective migration within curved multicellular tissues.

Overall, these studies highlight that individual and collective migration on complex curved surfaces remains poorly understood and could be more intricate than on flat 2D surfaces, exhibiting cell-type dependency, as observed in durotaxis[159]. In addition to migratory behaviour, the impact of curvature on cell proliferation remains unclear. For example, the proliferation of neural stem cells on the outer of convex nano-cylindrical wires increases with increasing curvature[160]. Epithelial proliferation within hollow sphere of constant curvature generates compressive stresses, deforming the elastic shell and resulting in a spontaneous tissue invagination[61], and the pressure accumulated due to cell proliferation in a confined area can inhibit cell-cycle progression[161].

Nuclear curvosensing and transcriptional regulation

Substrate curvature has been shown to induce cytoskeletal rearrangements that enable adherent cells to adapt to curvature changes while also modifying the transmission of forces to the nuclear membrane, ultimately resulting in changes to nuclear morphology and function. Understanding the mechanism of nuclear curvosensing remains a key open question in the field, particularly concerning how local changes in curvature influence transcriptional regulation.

Cytoskeletal tension exerts physical constraints on nuclei in convex regions, resulting in a pushing vertical force that leads to nuclear compression and flattened nuclear shapes (Fig. 5a). By contrast, nuclei experience a more relaxed mechanical state in concave zones, leading to a nuclear offset towards these regions (Fig. 5b). These results obtained on epithelial cells were confirmed with MSC, which translocates their nucleus from one concave region to another, avoiding convex regions[145].

Curvature-sensitive nuclear deformations can regulate the shuttling of transcriptional factors and proteins, such as Yes-associated protein (YAP), which has a role in cancer and other diseases[162,163]. The spatial distribution of YAP in epithelial cells is influenced by surface curvature via changes in nuclear shape and cell density[84]. These findings suggest a nuclear curvosensing mechanism that regulates nucleocytoplasmic shuttling, potentially influencing YAP-regulated processes and long-term gene expression. Interestingly, intestinal organoids cultured on curved hydrogels mimicking microvilli have shown that heterogeneities in YAP activities, governed by geometrically established gradients in cell mechanics, can determine villus and crypt domains[164]. A natural question that arises is: how can changes in substrate curvature impact nucleocytoplasmic transport proteins? Addressing this question is a crucial challenge for a better understanding of nuclear curvosensing mechanisms. However, it remains extremely complex, considering that mechanical forces act on nucleocytoplasmic transport with a

Glossary

Adherens junction
Component of the cell-cell junction in multicellular organisms in which cadherin receptors bridge neighbouring plasma membranes via their homophilic interactions. Adherens junction provides strong mechanical attachment between neighbouring cells through the linkage of their cytoplasmic face to the actin cytoskeleton.

BAR-domain protein
Highly conserved protein dimerization domains that occur in many proteins involved in membrane dynamics and act as connecting links between actin dynamics and membrane rearrangements in all eukaryotes. BAR domains preferentially bind to curved membrane regions.

Chromatin
Complex of genomic DNA with proteins called histones that forms chromosomes within the nucleus of eukaryotic cells.

Durotaxis
Guidance of cell migration by rigidity gradients, which arise from differential structural properties of the extracellular matrix. Most cells migrate up rigidity gradients (that is, in the direction of greater stiffness) but some cell types have been reported to migrate down rigidity gradients (known as negative durotaxis).

Epithelial tissues
Single-cell monolayers that separate tissues or cavities from their environment.

Filopodia
Slender and finger-like projections that extend from the leading edge of migrating cells. They are filled with bundled actin filaments and are involved in cell migration, cell-cell communication and sensing the environment.

Focal adhesions
Multiprotein site within cells that mechanically interact the extracellular matrix (cell outside) with the actin cytoskeleton (cell inside).

Gene transcription
Process of copying a segment of DNA sequence into an RNA molecule. This process can be divided in three steps: initiation, elongation and termination.

Histone
Family of positively charged proteins that associate with DNA and help condense it into chromatin.

Hypotonic shocks
Refer to an environmental medium that has a lower concentration of solutes than the cytoplasm, inducing a flow of water into the cell and a sudden modification of its osmotic pressure.

Lamellipodia
Thin projection that extends from the leading edge of a migrating cell and contains a quasi-2D actin mesh. These projections on the leading edge are involved in cell migration and exploration of the environment.

Laplace law
The pressure of a bubble with fixed surface tension varies inversely with its radius of curvature.

Manifold
A topological space M for which every point x has a neighbourhood homeomorphic to Euclidean space. In simple terms, it is a mathematical concept describing a space that appears flat similar to ordinary Euclidean space when you zoom in close enough but can have a more complicated overall shape such as a curved shaped.

Mechanosensing
Molecular process through which cells or cellular components translate mechanical forces or deformations into biochemical signals.

Mechanotransduction
Cellular responses to changes in the mechanical environment, including forces, deformations or mechanical properties.

Membrane tension
Local characteristic of the membrane, delineating the stretching-compression elastic stresses at each point along the membrane surface. This involves examining an infinitesimal element of the membrane plane, isolated by an imaginary boundary. Mechanical tension is the force exerted on the unit length of this imaginary boundary by the surrounding membrane, acting tangentially to the membrane plane.

Mesenchymal stem cells (MSCs)
Type of multipotent stromal cell that can differentiate into various cell types, such as osteoblasts (bone cells), chondrocytes (cartilage cells) and adipocytes (fat cells).

Microvilli
Finger-like projections of ~1–2 µm in length that extend from the surface of epithelial cells lining, for instance, the small intestine, kidney tubules and the inner ear. Microvilli are filled with bundled actin filaments and are involved in a wide variety of functions, including absorption, secretion, cellular adhesion and mechanotransduction.

Molecular clutch model
Concept that describes the flexible transmission of forces generated by the flow of actin filaments to adhesion sites, allowing cells to exert a spatially and temporally regulated grip on the substrate. It has a crucial role in the mechanical connection between the actin flow and cell adhesion complexes during cell migration.

Nematic order
Refers to a state of molecular alignment observed in cellular populations such as fibroblasts, akin to the alignment seen in liquid crystals. In this state, molecular entities exhibit a preferred directionality without long-range positional order.

Osmotic pressure
Pressure caused by a difference in the amounts of solutes (or molecules) between solutions (or fluids) separated by a semipermeable membrane.

Second harmonic generation microscopy
A second-order coherent process is employed, up-converting two lower energy photons precisely to twice the incident frequency (half the wavelength) of an excitation laser. This nonlinear imaging technique has proven effective in the specific and sensitive visualization of endogenous extracellular matrix components, such as collagen fibres, across diverse sample types.

Signal transduction
Process by which cells receive, interpret and respond to extracellular forces and signals. This intricate communication system involves the transmission of molecular signals through a series of events, ultimately leading to a cellular response or change in behaviour.

Tessellation
Repeating pattern that covers a 2D surface without overlaps or gaps using one or more geometric shapes, called tiles, with no overlaps and no gaps.

Transcription
Process by which the information in a strand of DNA is copied into a new molecule of messenger RNA.

Glossary (continued)

Vertex models
A class of mathematical models that treat cells as individual objects, represented by polygons in two dimensions and polyhedra in three dimensions. Epithelial tissues are modelled as a connected mesh of these polygons or polyhedral elements, and mechanical forces are applied to the vertices of these geometric structures.

Villus and crypt domains
Two distinct regions of the intestinal epithelium, which play important roles in nutrient uptake and tissue regeneration, respectively. The villus is a finger-like projection lined with absorptive enterocytes, secretory enteroendocrine cells and goblet cells. The crypt is a pocket-like invagination located at the base of the villus that houses the intestinal stem cell niche.

Viscoelasticity
Rheological property of biological tissues and materials that present elastic properties and viscous properties, which allow for timescale-dependent deformation when subjected to mechanical stress.

Yes-associated protein
Yes-associated protein, also known as YAP, is a mechanosensitive transcriptional co-activator protein that associates with several DNA-binding proteins to drive gene transcription. YAP activity is regulated by many kinase cascade pathways and proteins through phosphorylation. Phosphorylated YAP can be sequestered in the cytoplasm and then degraded by the ubiquitin-proteasome system, whereas unphosphorylated YAP translocates to the nucleus, where it performs a series of functions. YAP and its paralogue, transcriptional co-activator with PDZ-binding motif (TAZ), are the major downstream effectors of the Hippo pathway.

differential effect on passive and facilitated diffusion and a dependence on the molecular weight of a protein[165].

Remarkably, changes in curvature were also associated with differentiation patterns that correlated with modifications of the stress field. MSCs cultured on 2D sinusoidal adhesive bands differentiated into osteocytes at convex edges and adipocytes at concave edges, regardless of the band amplitude or thickness[166]. Traction force measurements revealed stress gradients preceding and mirroring differentiation patterns, with high stress favouring osteogenesis (Fig. 5a) and low stress promoting adipogenesis (Fig. 5b), demonstrating a role for mechanical forces in the emergence of patterns of cell differentiation[166]. Additional evidence confirmed that transcriptomic activity of MSCs is sensitive to curvature changes, leading to three processes: downregulation of a large subset of genes involved in stress, remodelling of the cytoskeleton and proliferation of cells[145]. MSCs on hemispherical caps exhibit higher levels of osteogenic differentiation markers[18] and Gaussian curvature has been suggested as a driving factor in osteogenic differentiation and bone regeneration[167].

The interplay between substrate curvature and cell differentiation was also investigated on other cell types and at larger curvature scales. For instance, myoblast transdifferentiation of keratocytes results in lower sensitivity of curvature[168], whereas milliscale concave curvature promotes differentiation of skeletal muscle cells[169]. Collectively, these studies support the emerging concept of nuclear curvosensing and indicate that mechanical adaptation of the nucleus to local changes in surface curvature can activate downstream signalling pathways and regulate transcription. However, the precise mechanism for direct sensing of curvature and converting mechanical forces generated by the cytoskeleton into transcriptional outputs remains elusive. A mechanical insight into the regulatory process of substrate curvature on stem cell fate was suggested based on studies of MSCs on concave substrates. Cell contractile forces in curved MSCs increase through the upregulation of phosphorylated light chains in myosin motors, leading to nuclear deformation that alters the histone modification profile and promotes differentiation of MSCs[170]. Further progress in unravelling the molecular details of the curvosensing mechanism and the curvoregulation of transcription in adherent cells will require dynamic investigations of substrate curvature modulation and visualization of cytoskeletal tension, chromatin compaction and nuclear mechanoadaptation in curved tissues.

Further progress in understanding the mechanism of curvoregulation of transcription in adherent cells will require dynamic investigations of substrate curvature modulation with live visualization of mechanical stress in curved epithelia[76] and the associated chromatin compaction.

Implications for human diseases

In vivo, cells dynamically adapt their morphology to the physicochemical properties of the surrounding fibrous matrix, which exhibits a large range of curved patterns across various length scales. There is evidence that alterations in tissue organization and specific cellular functions in response to curvature changes are characteristic features of numerous diseases. Notably, curvature has emerged as a pivotal factor in certain cancer types and has potential diagnosis implications. For instance, the local variations in the surface curvature of breast lesions extracted from tomography images can serve as a novel image feature for classifying breast tumours[171,172].

At a microscopic scale, emerging evidence suggests that interfacial curvature is implicated in the modulation of tumour morphogenesis and tumorigenicity[173,174]. However, additional matrix properties, such as stiffness[175], have been implicated in the severity of pancreatic, breast and prostate cancers. To investigate the interplay between interfacial curvature and matrix stiffness, micropatterned hydrogels with various geometries of adhesive islands were used to culture heterotypic cell populations[176]. Convex regions of the co-culture interface, corresponding to high stress regions, were found to activate cancer-associated fibroblasts, which adopted a myofibroblast phenotype. In addition to 2D investigations, tumour cells were cultured on

3D microenvironments with tunable stiffness and variable geometries encompassing concave and convex regions. Although it was found in vitro that convex curvature zones exhibit more cancer stem cell markers than concave zones[177], in vivo experiments have not definitely established whether the regulation of cancer cells is primarily influenced by curvature or solely by the presence of the interface. Collectively, these findings indicate that interfacial curvature can be considered as a biophysical cue in cancer development[82]. Nonetheless significant knowledge gaps remain regarding how interfacial curvature triggers cell tumorigenicity. Future studies should combine in vitro models with in vivo experiments to explore how subtle changes in convex and concave interfacial curvatures may guide tumorigenicity and epithelial–to–mesenchymal transition.

In addition to interfacial curvature, the role in tumorigenicity of the tissue curvature, such as in capillaries, ducts or lobes, remains an intriguing question. Recent in vivo experiments in mice, combined with in vitro experiments on organoids and histological observations of human pancreatic tissues, have shed light on the significance of tissue curvature in epithelial tumorigenesis[19]. Three–dimensional imaging of curved pancreatic tissues and vertex model simulations reveal that small pancreatic ducts produced exophytic growth (outward expansion from the duct), whereas large ducts undergo endophytic deformation (growth inward to the ductal lumen). This transition from exophytic to endophytic growth is attributed to a central mechanism involving a balance between apical and basal tensions. In small tubes, the imbalance between apical and basal tensions fails to overcome the epithelial resistance, resulting in outward lesion growth (exophytic behaviour). Conversely, large tubes exhibit transformed epithelial cells with cytoskeletal changes associated with increased basal tensions and decreased apical tensions, leading to inward lesion growth (endophytic behaviour). Interestingly, theoretical models based on the bending modulus of pancreatic tissues and changes in apico–basal tensions predict that the transition from exophytic to endophytic should occur at a mean tube radius of 10 μm (0.1 μm^{-1} in curvature)[19]. These findings have implications for studying other cancer types characterized by curved features such as cysts, ducts and crypts, including breast and ovarian cancers. Notably, it has been suggested that matrix curvature affecting tension in the epithelial monolayer could trigger the invasion of fallopian tube epithelial cells, which are trapped into cortical inclusion cysts[15].

Collectively, these studies emphasize the role of tissue curvature in human diseases, particularly in cancer development. They also demonstrate that cells integrate various physicochemical factors simultaneously, and alterations in the balance of cellular forces required to adapt to curvature changes can have dramatic consequences, promoting the emergence of a tumoural phenotype. To understand this intricate mechanism, it is crucial to elucidate how curvature length scales influence the interplay among interfacial energy, apico–basal tension and intercellular adhesion. Indeed, these factors have the potential to activate specific mechanotransduction pathways, thereby influencing and modulating the activity of transcriptional factors implicated in cancer, such as YAP/TAZ[178].

Outlook

Understanding the link among geometry, curvature and in–plane tension is crucial to better understand the initiation of fundamental processes such as gastrulation[179] and the mechanism of organ separation through folding dynamics[180]. Exploring the influence of curvature on topological transitions will also contribute to a better understanding of cellular rearrangements in curved tissues[82]. With this in mind, it is interesting to study more complex curved surfaces with positive, zero and negative Gaussian curvatures, as observed in toroidal structures[181].

Beyond the contribution of curvature to the formation of intricate biological structures, an increasing body of evidence indicates that it has a central role in fundamental cellular functions. For instance, it was suggested that the lung branching process is regulated by a feedback loop between tissue curvature and extracellular signal–regulated kinase (ERK) activity[182]. In addition, epithelial cell extrusion, which is involved in tissue homeostasis, is influenced differently by the sign of curvature through an osmotic process[183]. Despite significant progress in understanding of the impact of substrate curvature on specific biological processes, many questions remain unanswered.

One such question pertains to how cells dynamically perceive and adapt to modifications in curvature and how the mechanical signals originating from different length scales of curvature are transduced into specific biochemical responses. Although intriguing findings have emerged regarding the cytoskeletal reorganization in response to curvature changes, the mechanisms underlying the adaptation in space and time of the internal force balance remain unclear. To address this challenge, it is necessary to measure the temporal adaptation of cytoskeletal components and other subcellular structures to dynamic changes in surface curvature. Doing so is particularly important for understanding the regulation of the internal force balance, especially in terms of apico–basal tensions. Tools capable to dynamically modulate substrate curvature will be required to tackle this challenge[184]. Furthermore, the transmission of forces across the nucleocytoskeletal coupling in curved situations has yet to be thoroughly studied.

Despite the influence of cytoskeletal forces on the spatial arrangement of chromatin and the formation of condensed domains that regulate gene expression and cell fate determinations, it remains unclear how cells convey modulation of the apico–basal tension from the curved substrate to the nucleus to regulate gene expression. Using linker of nucleoskeleton and cytoskeleton complexes, adherent cells can generate forces on the nuclear lamina that affect the chromatin condensation state, implying a mechanical adaptation of the nucleus to local changes in surface curvature. Unravelling the complex mechanical interplay among curvature, substrate traction forces, internal cell force balance, cytoskeletal filaments, the nuclear envelope and chromatin state compaction will require interdisciplinary approaches in cell mechanobiology. Experimental methods incorporating stimuli–responsive biomaterials at different length scales, precise mechanical manipulation, co–culture of different cell types, genetic manipulation, live–cell imaging and optogenetics tools with high spatial and temporal resolution will be necessary. The development of biomaterials with multiscale curvature patterns that can dynamically respond to external stimuli over time is crucial. These materials have the potential to revolutionize the study of the dynamic interplay between cells and their changing microenvironment. For instance, they can be used to investigate how specific signalling pathways (such as YAP/TAZ, Ras/Erk and RhoA) are involved in curvosensing mechanisms. However, to fully realize their potential, new optogenetics tools are needed to control the spatiotemporal localization and activation of these signalling pathways. Such tools would enable researchers to better understand the complex signalling networks that govern the cellular response to curvature changes. These advanced experimental tools will allow addressing outstanding questions, such as how various organelles individually respond to the matrix curvature and cooperate to deliver a curvature–dependent transcriptional output. There are still other technological challenges to overcome to understand tissue adaptation

to curvature modulations, whether at the mechanical level (for example, by real-time observation of internal cellular tension in tissues) or at the functional level (by real-time observation of chromatin compaction and gene expression modifications). In addition to determining the physical laws that describe how the balance of mechanical forces in curved cells leads to transcriptional outputs, efforts should be directed towards translating in vitro techniques and deploying new molecular biosensors (strain gauges and optical and magnetic biosensors) in in vivo situations. Doing so will enable researchers to better understand the mechanisms behind tissue adaptation to curvature modulations, and help with developing more effective treatments for diseases that involve tissue deformation, such as cancer and cardiovascular disease.

These experimental breakthroughs will pave the way for mechanical models that provide a more integrated view, incorporating the roles of cell–substrate adhesions, the cell membrane, cytoskeletal filaments, nucleus and other organelles. Theoretical modelling will also be essential for exploring the complexity of the cooperative interactions between different organelles to various length scales of curvature and guiding the comprehensive analysis of complex interconnected experimental data sets.

Unravelling the interplay between mechanical and biochemical parameters will enable the elucidation of the mechanism of curvosensing and clarify which cellular mechanotransduction pathways are activated at specific length scales of curvature. This knowledge will also help determine the interplay between curvature and cell fate. Collectively, these efforts will enhance our fundamental understanding of the complex mechanisms by which tissues assemble into organs that utilize curvature to create functional architectures. Furthermore, these endeavours have the potential to guide the development of bioengineered tissues with advanced functions and lead to new translating and therapeutic strategies[185] for treating disrupted mechanotransduction pathways and human diseases that arise from changes in curvature.

Published online: 08 March 2024

References

1. Procès, A., Luciano, M., Kalukula, Y., Ris, L. & Gabriele, S. Multiscale mechanobiology in brain physiology and diseases. *Front. Cell Dev. Biol.* **10**, 823857 (2022).
2. Lantoine, J. et al. Matrix stiffness modulates formation and activity of neuronal networks of controlled architectures. *Biomaterials* **89**, 14-24 (2016).
3. Riaz, M., Versaevel, M., Mohammed, D., Glinel, K. & Gabriele, S. Persistence of fan-shaped keratocytes is a matrix-rigidity-dependent mechanism that requires α5β1 integrin engagement. *Sci. Rep.* **6**, 34141 (2016).
4. Saraswathibhatla, A., Indana, D. & Chaudhuri, O. Cell-extracellular matrix mechanotransduction in 3D. *Nat. Rev. Mol. Cell Biol.* **24**, 495-516 (2023).
5. Paul, C. D., Mistriotis, P. & Konstantopoulos, K. Cancer cell motility: lessons from migration in confined spaces. *Nat. Rev. Cancer* **17**, 131-140 (2017).
6. Mohammed, D. et al. Substrate area confinement is a key determinant of cell velocity in collective migration. *Nat. Phys.* **15**, 858-866 (2019).
7. Lomakin, A. J. et al. The nucleus acts as a ruler tailoring cell responses to spatial constraints. *Science* **370**, eaba2894 (2020).
8. Chaudhuri, O., Cooper-White, J., Janmey, P. A., Mooney, D. J. & Shenoy, V. B. Effects of extracellular matrix viscoelasticity on cellular behaviour. *Nature* **584**, 535-546 (2020).
9. Adu-Berchie, K. et al. Generation of functionally distinct T-cell populations by altering the viscoelasticity of their extracellular matrix. *Nat. Biomed. Eng.* **7**, 1374-1391 (2023).
10. Elosegui-Artola, A. et al. Matrix viscoelasticity controls spatiotemporal tissue organization. *Nat. Mater.* **22**, 117–127 (2023).
11. Trepat, X. et al. Universal physical responses to stretch in the living cell. *Nature* **447**, 592-595 (2007).
12. Bruyère, C. et al. Actomyosin contractility scales with myoblast elongation and enhances differentiation through YAP nuclear export. *Sci. Rep.* **9**, 15565 (2019).
13. Martino, F., Perestrelo, A. R., Vinarský, V., Pagliari, S. & Forte, G. Cellular mechanotransduction: from tension to function. *Front. Physiol.* **9**, 824 (2018).
14. Lantoine, J. et al. Inflammatory molecules released by mechanically injured astrocytes trigger presynaptic loss in cortical neuronal networks. *ACS Chem. Neurosci.* **12**, 3885-3897 (2021).
15. Fleszar, A. J., Walker, A., Kreeger, P. K. & Notbohm, J. Substrate curvature induces fallopian tube epithelial cell invasion via cell-cell tension in a model of ovarian cortical inclusion cysts. *Integr. Biol.* **11**, 342-352 (2019).
16. Maechler, F. A., Allier, C., Roux, A. & Tomba, C. Curvature-dependent constraints drive remodeling of epithelia. *J. Cell Sci.* **132**, jcs222372 (2019).
17. Mandrycky, C., Hadland, B. & Zheng, Y. 3D curvature-instructed endothelial flow response and tissue vascularization. *Sci. Adv.* **6**, eabb3629 (2020).
18. Werner, M. et al. Surface curvature differentially regulates stem cell migration and differentiation via altered attachment morphology and nuclear deformation. *Adv. Sci.* **4**, 1600347 (2017).
19. Messal, H. A. et al. Tissue curvature and apicobasal mechanical tension imbalance instruct cancer morphogenesis. *Nature* **566**, 126–130 (2019).
20. Luciano, M. et al. Appreciating the role of cell shape changes in the mechanobiology of epithelial tissues. *Biophys. Rev.* **3**, 011305 (2022).
21. Mohammed, D. et al. Innovative tools for mechanobiology: unravelling outside-in and inside-out mechanotransduction. *Front. Bioeng. Biotechnol.* **7**, 162 (2019).
22. Basu, R., Munteanu, E. L. & Chang, F. Role of turgor pressure in endocytosis in fission yeast. *Mol. Biol. Cell* **25**, 549-727 (2014).
23. Roffay, C. et al. Passive coupling of membrane tension and cell volume during active response of cells to osmosis. *Proc. Natl Acad. Sci. USA* **118**, e2103228118 (2021).
24. Latorre, E. et al. Active superelasticity in three-dimensional epithelia of controlled shape. *Nature* **563**, 203-208 (2018).
25. Jentsch, T. J., Lutter, D., Planells-Cases, R., Ullrich, F. & Voss, F. K. VRAC: molecular identification as LRRC8 heteromers with differential functions. *Pflug. Arch. Eur. J. Physiol.* **468**, 385-393 (2016).
26. Houdusse, A. & Sweeney, H. L. How myosin generates force on actin filaments. *Trends Biochem. Sci.* **41**, 989-997 (2016).
27. Hill, T. L. & Kirschner, M. W. Bioenergetics and kinetics of microtubule and actin filament assembly-disassembly. *Int. Rev. Cytol.* **78**, 1-125 (1982).
28. Molodtsov, M. I., Grishchuk, E. L., Efremov, A. K., McIntosh, J. R. & Ataullakhanov, F. I. Force production by depolymerizing microtubules: a theoretical study. *Proc. Natl Acad. Sci. USA* **102**, 4353-4358 (2005).
29. Matis, M. The mechanical role of microtubules in tissue remodeling. *BioEssays* **42**, 1900244 (2020).
30. Kozlov, M. M. & Chernomordik, L. V. Membrane tension and membrane fusion. *Curr. Opin. Struct. Biol.* **33**, 61-67 (2015).
31. Gibbs, J. W. *The Scientific Papers of J. Willard Gibbs* (Dover Publications, Inc., 1961).
32. De Belly, H. et al. Actin-driven protrusions generate rapid long-range membrane tension propagation in cells. Preprint at *bioRxiv* https://doi.org/10.1101/2022.09.07.507005 (2022).
33. Lieber, A. D., Yehudai-Resheff, S., Barnhart, E. L., Theriot, J. A. & Keren, K. Membrane tension in rapidly moving cells is determined by cytoskeletal forces. *Curr. Biol.* **23**, 1409-1417 (2013).
34. Mueller, J. et al. Load adaptation of lamellipodial actin networks. *Cell* **171**, 188-200.e16 (2017).
35. Hetmanski, J. H. R. et al. Membrane tension orchestrates rear retraction in matrix-directed cell migration. *Dev. Cell* **51**, 460-475.e10 (2019).
36. Taubenberger, A. V., Baum, B. & Matthews, H. K. The mechanics of mitotic cell rounding. *Front. Cell Dev. Biol.* **8**, 687 (2020).
37. Sedzinski, J. et al. Polar actomyosin contractility destabilizes the position of the cytokinetic furrow. *Nature* **476**, 462-466 (2011).
38. Bertet, C., Sulak, L. & Lecuit, T. Myosin-dependent junction remodelling controls planar cell intercalation and axis elongation. *Nature* **429**, 667-671 (2004).
39. Kruse, K., Joanny, J. F., Jülicher, F., Prost, J. & Sekimoto, K. Generic theory of active polar gels: a paradigm for cytoskeletal dynamics. *Eur. Phys. J. E* **16**, 5-16 (2005).
40. Berezney, J., Goode, B. L., Fraden, S. & Dogic, Z. Extensile to contractile transition in active microtubule-actin composites generates layered asters with programmable lifetimes. *Proc. Natl Acad. Sci. USA* **119**, e2115895119 (2022).
41. Saw, T. B. et al. Topological defects in epithelia govern cell death and extrusion. *Nature* **544**, 212-216 (2017).
42. Blanch-Mercader, C., Guillamat, P., Roux, A. & Kruse, K. Quantifying material properties of cell monolayers by analyzing integer topological defects. *Phys. Rev. Lett.* **126**, 028101 (2021).
43. Blanch-Mercader, C., Guillamat, P., Roux, A. & Kruse, K. Integer topological defects of cell monolayers: mechanics and flows. *Phys. Rev. E* **103**, 012405 (2021).
44. Balasubramaniam, L. et al. Investigating the nature of active forces in tissues reveals how contractile cells can form extensile monolayers. *Nat. Mater.* **20**, 1156–1166 (2021).
45. Dumortier, J. G. et al. Hydraulic fracturing and active coarsening position the lumen of the mouse blastocyst. *Science* **365**, 465-468 (2019).
46. Kosmalska, A. J. et al. Physical principles of membrane remodelling during cell mechanoadaptation. *Nat. Commun.* **6**, 7292 (2015).
47. Dietrich, J.-E. & Hiiragi, T. Stochastic patterning in the mouse pre-implantation embryo. *Development* **134**, 4219-4231 (2007).
48. Rhumbler, L. Zur Mechanik des Gastrulationsvorganges insbesondere der Invagination: Eine entwickelungsmechanische Studie. *Arch. Für. Entwickl. Org.* **14**, 401-476 (1902).
49. Moore, A. R. & Burt, A. S. On the locus and nature of the forces causing gastrulation in the embryos of *Dendraster excentricus*. *J. Exp. Zool.* **82**, 159-171 (1939).
50. Martin, A. C. & Goldstein, B. Apical constriction: themes and variations on a cellular mechanism driving morphogenesis. *Development* **141**, 1987-1998 (2014).

51. Gilmour, D., Rembold, M. & Leptin, M. From morphogen to morphogenesis and back. *Nature* **541**, 311-320 (2017).
52. Pérez-González, C. et al. Mechanical compartmentalization of the intestinal organoid enables crypt folding and collective cell migration. *Nat. Cell Biol.* **23**, 745-757 (2021).
53. Yang, Q. et al. Cell fate coordinates mechano-osmotic forces in intestinal crypt formation. *Nat. Cell Biol.* **23**, 733-744 (2021).
54. Haas, P. A. & Goldstein, R. E. Morphoelasticity of large bending deformations of cell sheets during development. *Phys. Rev. E* **103**, 022411 (2021).
55. Höhn, S., Honerkamp-Smith, A. R., Haas, P. A., Trong, P. K. & Goldstein, R. E. Dynamics of a *Volvox* embryo turning itself inside out. *Phys. Rev. Lett.* **114**, 178101 (2015).
56. Collinet, C. & Lecuit, T. Programmed and self-organized flow of information during morphogenesis. *Nat. Rev. Mol. Cell Biol.* **22**, 245-265 (2021).
57. Münster, S. et al. Attachment of the blastoderm to the vitelline envelope affects gastrulation of insects. *Nature* **568**, 395-399 (2019).
58. Merzouki, A., Malaspinas, O., Trushko, A., Roux, A. & Chopard, B. Influence of cell mechanics and proliferation on the buckling of simulated tissues using a vertex model. *Nat. Comput.* **17**, 511-519 (2018).
59. Rauzi, M., Hočevar Brezavšček, A., Ziherl, P. & Leptin, M. Physical models of mesoderm invagination in *Drosophila* embryo. *Biophys. J.* **105**, 3-10 (2013).
60. Hannezo, E., Prost, J. & Joanny, J.-F. Instabilities of monolayered epithelia: shape and structure of villi and crypts. *Phys. Rev. Lett.* **107**, 078104 (2011).
61. Trushko, A. et al. Buckling of an epithelium growing under spherical confinement. *Dev. Cell* **54**, 655-668.e6 (2020).
62. Tozluoğlu, M. et al. Planar differential growth rates initiate precise fold positions in complex epithelia. *Dev. Cell* **51**, 299-312.e4 (2019).
63. Hughes, A. J. et al. Engineered tissue folding by mechanical compaction of the mesenchyme. *Dev. Cell* **44**, 165-178 (2018).
64. Jain, S. et al. The role of single-cell mechanical behaviour and polarity in driving collective cell migration. *Nat. Phys.* **16**, 802-809 (2020).
65. Guillamat, P., Blanch-Mercader, C., Pernollet, G., Kruse, K. & Roux, A. Integer topological defects organize stresses driving tissue morphogenesis. *Nat. Mater.* **21**, 588-597 (2022).
66. Bell, S., Lin, S.-Z., Rupprecht, J.-F. & Prost, J. Active nematic flows over curved surfaces. *Phys. Rev. Lett.* **129**, 118001 (2022).
67. Fouchard, J. et al. Curling of epithelial monolayers reveals coupling between active bending and tissue tension. *Proc. Natl Acad. Sci. USA* **117**, 9377-9383 (2020).
68. Blonski, S. et al. Direction of epithelial folding defines impact of mechanical forces on epithelial state. *Dev. Cell* **56**, 3222-3234.e6 (2021).
69. Tomba, C., Luchnikov, V., Barberi, L., Blanch-Mercader, C. & Roux, A. Epithelial cells adapt to curvature induction via transient active osmotic swelling. *Dev. Cell* **57**, 1257–1270.e5 (2022).
70. Gómez-González, M., Latorre, E., Arroyo, M. & Trepat, X. Measuring mechanical stress in living tissues. *Nat. Rev. Phys.* **2**, 300-317 (2020).
71. Mehlenbacher, R. D., Kolbl, R., Lay, A. & Dionne, J. A. Nanomaterials for in vivo imaging of mechanical forces and electrical fields. *Nat. Rev. Mater.* **3**, 17080 (2018).
72. Tambe, D. T. et al. Monolayer stress microscopy: limitations, artifacts, and accuracy of recovered intercellular stresses. *PLoS ONE* **8**, e55172 (2013).
73. Trepat, X. et al. Physical forces during collective cell migration. *Nat. Phys.* **5**, 426-430 (2009).
74. Ng, M. R., Besser, A., Brugge, J. S. & Danuser, G. Mapping the dynamics of force transduction at cell-cell junctions of epithelial clusters. *eLife* **3**, e03282 (2014).
75. Vercruysse, E. et al. Geometry-driven migration efficiency of autonomous epithelial cell clusters. Preprint at *bioRxiv* https://doi.org/10.1101/2022.07.17.500364 (2022).
76. Marín-Llauradó, A. et al. Mapping mechanical stress in curved epithelia of designed size and shape. *Nat. Commun.* **14**, 4014 (2023).
77. Mughal, A., Cox, S. J., Weaire, D., Burke, S. R. & Hutzler, S. Demonstration and interpretation of 'scutoid' cells formed in a quasi-2D soap froth. *Philos. Mag. Lett.* **98**, 358-364 (2018).
78. Gómez-Gálvez, P., Vicente-Munuera, P., Anbari, S., Buceta, J. & Escudero, L. M. The complex three-dimensional organization of epithelial tissues. *Development* **148**, dev195669 (2021).
79. Gómez-Gálvez, P. et al. Scutoids are a geometrical solution to three-dimensional packing of epithelia. *Nat. Commun.* **9**, 2960 (2018).
80. Gómez, H. F., Dumond, M. S., Hodel, L., Vetter, R. & Iber, D. 3D cell neighbour dynamics in growing pseudostratified epithelia. *eLife* **10**, e68135 (2021).
81. Rupprecht, J.-F. et al. Geometric constraints alter cell arrangements within curved epithelial tissues. *MBoC* **28**, 3582-3594 (2017).
82. Lou, Y., Rupprecht, J.-F., Theis, S., Hiraiwa, T. & Saunders, T. E. Curvature-induced cell rearrangements in biological tissues. *Phys. Rev. Lett.* **130**, 108401 (2023).
83. Hannezo, E., Prost, J. & Joanny, J.-F. Theory of epithelial sheet morphology in three dimensions. *Proc. Natl Acad. Sci. USA* **111**, 27-32 (2014).
84. Luciano, M. et al. Cell monolayers sense curvature by exploiting active mechanics and nuclear mechanoadaptation. *Nat. Phys.* **17**, 1382-1390 (2021).
85. Odell, G. M., Oster, G., Alberch, P. & Burnside, B. The mechanical basis of morphogenesis. *Dev. Biol.* **85**, 446-462 (1981).
86. Fletcher, A. G., Osterfield, M., Baker, R. E. & Shvartsman, S. Y. Vertex models of epithelial morphogenesis. *Biophys. J.* **106**, 2291-2304 (2014).
87. Honda, H. & Eguchi, G. How much does the cell boundary contract in a monolayered cell sheet? *J. Theor. Biol.* **84**, 575-588 (1980).
88. Nagai, T. & Honda, H. A dynamic cell model for the formation of epithelial tissues. *Philos. Mag. Pt B* **81**, 699-719 (2001).
89. Farhadifar, R., Röper, J.-C., Aigouy, B., Eaton, S. & Jülicher, F. The influence of cell mechanics, cell-cell interactions, and proliferation on epithelial packing. *Curr. Biol.* **17**, 2095-2104 (2007).
90. Hočevar Brezavšček, A., Rauzi, M., Leptin, M. & Ziherl, P. A model of epithelial invagination driven by collective mechanics of identical cells. *Biophys. J.* **103**, 1069-1077 (2012).
91. Sumi, A. et al. Adherens junction length during tissue contraction is controlled by the mechanosensitive activity of actomyosin and junctional recycling. *Dev. Cell* **47**, 453-463. e3 (2018).
92. Théry, M., Pépin, A., Dressaire, E., Chen, Y. & Bornens, M. Cell distribution of stress fibres in response to the geometry of the adhesive environment. *Cell Motil. Cytoskelet.* **63**, 341-355 (2006).
93. Chen, C. S., Mrksich, M., Huang, S., Whitesides, G. M. & Ingber, D. E. Geometric control of cell life and death. *Science* **276**, 1425 (1997).
94. Thery, M. et al. Anisotropy of cell adhesive microenvironment governs cell internal organization and orientation of polarity. *Proc. Natl Acad. Sci. USA* **103**, 19771-19776 (2006).
95. Parker, K. K. et al. Directional control of lamellipodia extension by constraining cell shape and orienting cell tractional forces. *FASEB J.* **16**, 1195-1204 (2002).
96. Versaevel, M., Grevesse, T. & Gabriele, S. Spatial coordination between cell and nuclear shape within micropatterned endothelial cells. *Nat. Commun.* **3**, 671 (2012).
97. Senger, F. et al. Spatial integration of mechanical forces by α-actinin establishes actin network symmetry. *J. Cell Sci.* **132**, jcs236604 (2019).
98. Kilian, K. A., Bugarija, B., Lahn, B. T. & Mrksich, M. Geometric cues for directing the differentiation of mesenchymal stem cells. *Proc. Natl Acad. Sci. USA* **107**, 4872-4877 (2010).
99. McBeath, R., Pirone, D. M., Nelson, C. M., Bhadriraju, K. & Chen, C. S. Cell shape, cytoskeletal tension, and RhoA regulate stem cell lineage commitment. *Dev. Cell* **6**, 483-495 (2004).
100. Bischofs, I. B., Klein, F., Lehnert, D., Bastmeyer, M. & Schwarz, U. S. Filamentous network mechanics and active contractility determine cell and tissue shape. *Biophys. J.* **95**, 3488-3496 (2008).
101. Schakenraad, K. et al. Mechanical interplay between cell shape and actin cytoskeleton organization. *Soft Matter* **16**, 6328-6343 (2020).
102. James, J., Goluch, E. D., Hu, H., Liu, C. & Mrksich, M. Subcellular curvature at the perimeter of micropatterned cells influences lamellipodial distribution and cell polarity. *Cell Motil. Cytoskelet.* **65**, 841-852 (2008).
103. Vignaud, T., Blanchoin, L. & Théry, M. Directed cytoskeleton self-organization. *Trends Cell Biol.* **22**, 671-682 (2012).
104. Ladoux, B., Mège, R.-M. & Trepat, X. Front-rear polarization by mechanical cues: from single cells to tissues. *Trends Cell Biol.* **26**, 420-433 (2016).
105. Lam, N. T., Muldoon, T. J., Quinn, K. P., Rajaram, N. & Balachandran, K. Valve interstitial cell contractile strength and metabolic state are dependent on its shape. *Integr. Biol.* **8**, 1079-1089 (2016).
106. Gupta, S. K., Li, Y. & Guo, M. Anisotropic mechanics and dynamics of a living mammalian cytoplasm. *Soft Matter* **15**, 190-199 (2019).
107. Chen, T. et al. Large-scale curvature sensing by directional actin flow drives cellular migration mode switching. *Nat. Phys.* **15**, 393-402 (2019).
108. Anon, E. et al. Cell crawling mediates collective cell migration to close undamaged epithelial gaps. *Proc. Natl Acad. Sci. USA* **109**, 10891-10896 (2012).
109. Begnaud, S., Chen, T., Delacour, D., Mège, R.-M. & Ladoux, B. Mechanics of epithelial tissues during gap closure. *Curr. Opin. Cell Biol.* **42**, 52-62 (2016).
110. Ravasio, A. et al. Gap geometry dictates epithelial closure efficiency. *Nat. Commun.* **6**, 7683 (2015).
111. Sandu, G. et al. Kinked silicon nanowires: superstructures by metal-assisted chemical etching. *Nano Lett.* **19**, 7681-7690 (2019).
112. Huang, J. et al. Impact of order and disorder in RGD nanopatterns on cell adhesion. *Nano Lett.* **9**, 1111-1116 (2009).
113. Arnold, M. et al. Activation of integrin function by nanopatterned adhesive interfaces. *ChemPhysChem* **5**, 383-388 (2004).
114. Oria, R. et al. Force loading explains spatial sensing of ligands by cells. *Nature* **552**, 219-224 (2017).
115. Schaumann, E. N. & Tian, B. Actin-packed topography: cytoskeletal response to curvature. *Proc. Natl Acad. Sci. USA* **116**, 22897-22898 (2019).
116. Carey, S. P. et al. Local extracellular matrix alignment directs cellular protrusion dynamics and migration through Rac1 and FAK. *Integr. Biol.* **8**, 821-835 (2016).
117. Kennedy, K. M., Bhaw-Luximon, A. & Jhurry, D. Cell-matrix mechanical interaction in electrospun polymeric scaffolds for tissue engineering: implications for scaffold design and performance. *Acta Biomater.* **50**, 41-55 (2017).
118. Koons, B. et al. Cancer protrusions on a tightrope: nanofiber curvature contrast quantitates single protrusion dynamics. *ACS Nano* **11**, 12037–12048 (2017).
119. Mukherjee, A., Behkam, B. & Nain, A. S. Cancer cells sense fibers by coiling on them in a curvature-dependent manner. *iScience* **19**, 905-915 (2019).
120. Zhang, W. et al. Curved adhesions mediate cell attachment to soft matrix fibres in three dimensions. *Nat. Cell Biol.* **25**, 1453-1464 (2023).
121. Weiss, P. Experiments on cell and axon orientation in vitro: the role of colloidal exudates in tissue organization. *J. Exp. Zool.* **100**, 353-386 (1945).

122. Dunn, G. A. & Heath, J. P. A new hypothesis of contact guidance in tissue cells. *Exp. Cell Res.* **101**, 1-14 (1976).
123. Bade, N. D., Kamien, R. D., Assoian, R. K. & Stebe, K. J. Curvature and Rho activation differentially control the alignment of cells and stress fibers. *Sci. Adv.* **3**, e1700150 (2017).
124. Iruela-Arispe, M. L. & Davis, G. E. Cellular and molecular mechanisms of vascular lumen formation. *Dev. Cell* **16**, 222–231 (2009).
125. Sims, D. E. The pericyte – a review. *Tissue Cell* **18**, 153-174 (1986).
126. O'Connor, C., Brady, E., Zheng, Y., Moore, E. & Stevens, K. R. Engineering the multiscale complexity of vascular networks. *Nat. Rev. Mater.* **7**, 702-716 (2022).
127. Yu, S.-M. Substrate curvature affects the shape, orientation, and polarization of renal epithelial cells. *Acta Biomater.* **77**, 311-321 (2018).
128. Biton, Y. Y. & Safran, S. A. The cellular response to curvature-induced stress. *Phys. Biol.* **6**, 046010 (2009).
129. Bade, N. D., Xu, T., Kamien, R. D., Assoian, R. K. & Stebe, K. J. Gaussian curvature directs stress fiber orientation and cell migration. *Biophys. J.* **114**, 1467–1476 (2018).
130. Kemkemer, R., Teichgräber, V., Schrank-Kaufmann, S., Kaufmann, D. & Gruler, H. Nematic order-disorder state transition in a liquid crystal analogue formed by oriented and migrating amoeboid cells. *Eur. Phys. J. E* **3**, 101-110 (2000).
131. Duclos, G., Garcia, S., Yevick, H. G. & Silberzan, P. Perfect nematic order in confined monolayers of spindle-shaped cells. *Soft Matter* **10**, 2346-2353 (2014).
132. Harmand, N., Huang, A. & Hénon, S. 3D shape of epithelial cells on curved substrates. *Phys. Rev. X* **11**, 031028 (2021).
133. Harmand, N., Dervaux, J., Poulard, C. & Hénon, S. Thickness of epithelia on wavy substrates: measurements and continuous models. *Eur. Phys. J. E* **45**, 53 (2022).
134. Werner, M., Kurniawan, N. A., Korus, G., Bouten, C. V. C. & Petersen, A. Mesoscale substrate curvature overrules nanoscale contact guidance to direct bone marrow stromal cell migration. *J. R. Soc. Interface* **15**, 20180162 (2018).
135. Asano, N., Sugihara, S., Suye, S. & Fujita, S. Electrospun porous nanofibers with imprinted patterns induced by phase separation of immiscible polymer blends. *ACS Omega* **7**, 19997–20005 (2022).
136. Kumbar, S. G., Nukavarapu, S. P., James, R., Nair, L. S. & Laurencin, C. T. Electrospun poly(lactic acid-co-glycolic acid) scaffolds for skin tissue engineering. *Biomaterials* **29**, 4100-4107 (2008).
137. Bowers, D. T. & Brown, J. L. Nanofiber curvature with Rho GTPase activity increases mouse embryonic fibroblast random migration velocity. *Integr. Biol.* **13**, 295-308 (2021).
138. Qu, J. et al. Optimization of electrospun TSF nanofiber alignment and diameter to promote growth and migration of mesenchymal stem cells. *Appl. Surf. Sci.* **261**, 320-326 (2012).
139. DiMilla, P., Stone, J., Quinn, J., Albelda, S. & Lauffenburger, D. Maximal migration of human smooth muscle cells on fibronectin and type IV collagen occurs at an intermediate attachment strength. *J. Cell Biol.* **122**, 729-737 (1993).
140. Parsons, J. T., Horwitz, A. R. & Schwartz, M. A. Cell adhesion: integrating cytoskeletal dynamics and cellular tension. *Nat. Rev. Mol. Cell Biol.* **11**, 633-643 (2010).
141. Schreiber, C., Amiri, B., Heyn, J. C. J., Rädler, J. O. & Falcke, M. On the adhesion-velocity relation and length adaptation of motile cells on stepped fibronectin lanes. *Proc. Natl Acad. Sci. USA* **118**, e2009959118 (2021).
142. Badami, A. S., Kreke, M. R., Thompson, M. S., Riffle, J. S. & Goldstein, A. S. Effect of fiber diameter on spreading, proliferation, and differentiation of osteoblastic cells on electrospun poly(lactic acid) substrates. *Biomaterials* **27**, 596-606 (2006).
143. Tian, F. et al. Quantitative analysis of cell adhesion on aligned micro- and nanofibers. *J. Biomed. Mater. Res.* **84A**, 291-299 (2008).
144. Noriega, S. E., Hasanova, G. I., Schneider, M. J., Larsen, G. F. & Subramanian, A. Effect of fiber diameter on the spreading, proliferation and differentiation of chondrocytes on electrospun chitosan matrices. *Cell Tissues Organs* **195**, 207-221 (2012).
145. Pieuchot, L. et al. Curvotaxis directs cell migration through cell-scale curvature landscapes. *Nat. Commun.* **9**, 3995 (2018).
146. Werner, M., Petersen, A., Kurniawan, N. A. & Bouten, C. V. C. Cell-perceived substrate curvature dynamically coordinates the direction, speed, and persistence of stromal cell migration. *Adv. Biosys.* **3**, 1900080 (2019).
147. He, X. & Jiang, Y. Substrate curvature regulates cell migration. *Phys. Biol.* **14**, 035006 (2017).
148. Hegarty-Cremer, S. G. D., Simpson, M. J., Andersen, T. L. & Buenzli, P. R. Modelling cell guidance and curvature control in evolving biological tissues. *J. Theor. Biol.* **520**, 110658 (2021).
149. Yevick, H. G., Duclos, G., Bonnet, I. & Silberzan, P. Architecture and migration of an epithelium on a cylindrical wire. *Proc. Natl Acad. Sci. USA* **112**, 5944-5949 (2015).
150. Xi, W., Sonam, S., Lim, C. T. & Ladoux, B. Tubular microscaffolds for studying collective cell migration. in *Methods in Cell Biology* Vol. 146, 3-21 (Elsevier, 2018).
151. Ye, M. et al. Brain microvascular endothelial cells resist elongation due to curvature and shear stress. *Sci. Rep.* **4**, 4681 (2014).
152. Rougerie, P. et al. Topographical curvature is sufficient to control epithelium elongation. *Sci. Rep.* **10**, 14784 (2020).
153. Bidan, C. M. et al. How linear tension converts to curvature: geometric control of bone tissue growth. *PLoS ONE* **7**, e36336 (2012).
154. Ehrig, S. et al. Surface tension determines tissue shape and growth kinetics. *Sci. Adv.* **5**, 7 (2019).
155. Tambe, D. T. et al. Collective cell guidance by cooperative intercellular forces. *Nat. Mater.* **10**, 469-475 (2011).
156. Glentis, A. et al. The emergence of spontaneous coordinated epithelial rotation on cylindrical curved surfaces. *Sci. Adv.* **8**, eabn5406 (2022).
157. Brandstätter, T. Curvature induces active velocity waves in rotating spherical tissues. *Nat. Commun.* **14**, (2023).
158. Luciano, M., Versaevel, M., Kalukula, Y. & Gabriele, S. Mechanoresponse of curved epithelial monolayers lining bowl-shaped 3D microwells. *Adv. Healthc. Mater.* **13**, 2203377 (2024).
159. Shellard, A. & Mayor, R. Durotaxis: the hard path from in vitro to in vivo. *Dev. Cell* **56**, 227-239 (2021).
160. Christopherson, G. T., Song, H. & Mao, H.-Q. The influence of fiber diameter of electrospun substrates on neural stem cell differentiation and proliferation. *Biomaterials* **30**, 556-564 (2009).
161. Di Meglio, I. et al. Pressure and curvature control of the cell cycle in epithelia growing under spherical confinement. *Cell Rep.* **40**, 111227 (2022).
162. Elosegui-Artola, A. et al. Force triggers YAP nuclear entry by regulating transport across nuclear pores. *Cell* **171**, 1397–1410.e14 (2017).
163. Kalukula, Y., Stephens, A. D., Lammerding, J. & Gabriele, S. Mechanics and functional consequences of nuclear deformations. *Nat. Rev. Mol. Cell Biol.* **23**, 583-602 (2022).
164. Gjorevski, N. et al. Tissue geometry drives deterministic organoid patterning. *Science* **375**, eaaw9021 (2022).
165. Andreu, I. Mechanical force application to the nucleus regulates nucleocytoplasmic transport. *Nat. Cell Biol.* **24**, 896-905 (2022).
166. Ruiz, S. A. Emergence of patterned stem cell differentiation within multicellular structures. *Stem Cell* **26**, 2921-2927 (2008).
167. Yang, Y. et al. Gaussian curvature-driven direction of cell fate toward osteogenesis with triply periodic minimal surface scaffolds. *Proc. Natl Acad. Sci. USA* **119**, e2206684119 (2022).
168. Van der Putten, C., van den Broek, D. & Kurniawan, N. A. Myofibroblast transdifferentiation of keratocytes results in slower migration and lower sensitivity to mesoscale curvatures. *Front. Cell Dev. Biol.* **10**, 930373 (2022).
169. Connon, C. J. & Gouveia, R. M. Milliscale substrate curvature promotes myoblast self-organization and differentiation. *Adv. Biol.* **5**, e2000280 (2021).
170. Xu, X. et al. Histone modification of osteogenesis related genes triggered by substrate topography promotes human mesenchymal stem cell differentiation. *ACS Appl. Mater. Interfaces* **15**, 29752-29766 (2023).
171. Lee, J., Nishikawa, R. M., Reiser, I., Boone, J. M. & Lindfors, K. K. Local curvature analysis for classifying breast tumors: preliminary analysis in dedicated breast CT: local curvature analysis for classifying breast tumors. *Med. Phys.* **42**, 5479-5489 (2015).
172. Tan, S. et al. Adaptive region-growing with maximum curvature strategy for tumor segmentation in ^{18}F-FDG PET. *Phys. Med. Biol.* **62**, 5383-5402 (2017).
173. Arvanitis, C., Khuon, S., Spann, R., Ridge, K. M. & Chew, T.-L. Structure and biomechanics of the endothelial transcellular circumferential invasion array in tumor invasion. *PLoS ONE* **9**, e89758 (2014).
174. Zhu, P. et al. Biomechanical microenvironment regulates fusogenicity of breast cancer cells. *ACS Biomater. Sci. Eng.* **5**, 3817-3827 (2019).
175. Wullkopf, L. et al. Cancer cells' ability to mechanically adjust to extracellular matrix stiffness correlates with their invasive potential. *Mol. Biol. Cell* **29**, 2378-2385 (2018).
176. Nemec, S. et al. Interfacial curvature in confined coculture directs stromal cell activity with spatial corralling of pancreatic cancer cells. *Adv. Biol.* **5**, 2000525 (2021).
177. Lee, J., Abdeen, A. A., Wycislo, K. L., Fan, T. M. & Kilian, K. A. Interfacial geometry dictates cancer cell tumorigenicity. *Nat. Mater.* **15**, 856-862 (2016).
178. Franklin, J. M. Insights into recent findings and clinical application of YAP and TAZ in cancer. *Nat. Rev. Cancer* **23**, 512-525 (2023).
179. Fierling, J. et al. Embryo-scale epithelial buckling forms a propagating furrow that initiates gastrulation. *Nat. Commun.* **13**, 3348 (2022).
180. Villedieu, A. et al. Homeotic compartment curvature and tension control spatiotemporal folding dynamics. *Nat. Commun.* **14**, 594 (2023).
181. Wang, T., Dai, Z., Potier-Ferry, M. & Xu, F. Curvature-regulated multiphase patterns in tori. *Phys. Rev. Lett.* **130**, 048201 (2023).
182. Hirashima, T. & Matsuda, M. ERK-mediated curvature feedback regulates branch. *Morphogene. Lung Epithel. Tissue* https://doi.org/10.1101/2021.07.11.451982 (2021).
183. Huang, C.-K., Yong, X., She, D. T. & Teck, C. Surface curvature and basal hydraulic stress induce spatial bias in cell extrusion. https://doi.org/10.1101/2022.04.01.486717 (2022).
184. Roy, A. et al. Programmable tissue folding patterns in structured hydrogels. *Adv. Mater.* https://doi.org/10.1002/adma.202300017 (2023).
185. Kalukula, Y., Luciano, M. & Gabriele, S. Translating cell mechanobiology and nuclear deformations to the clinic. *Clin. Trans. Med.* **12**, e1000 (2022).
186. Doostmohammadi, A. & Ladoux, B. Physics of liquid crystals in cell biology. *Trends Cell Biol.* **32**, 140-150 (2022).
187. Lou, H.-Y. et al. Membrane curvature underlies actin reorganization in response to nanoscale surface topography. *Proc. Natl Acad. Sci. USA* **116**, 23143-23151 (2019).
188. Wagstyl, K. et al. BigBrain 3D atlas of cortical layers: cortical and laminar thickness gradients diverge in sensory and motor cortices. *PLoS Biol.* **18**, e3000678 (2020).
189. Conrad, L. et al. The biomechanical basis of biased epithelial tube elongation in lung and kidney development. *Development* **148**, dev194209 (2021).
190. Mederacke, M., Conrad, L., Vetter, R. & Iber, D. Geometric effects position renal vesicles during kidney development. *Cell Rep.* https://doi.org/10.1101/2022.08.30.505859 (2022).

191. Peurla, M. et al. Morphometric analysis of the terminal ductal lobular unit architecture in human breast. Preprint at *bioRxiv* https://doi.org/10.1101/2023.03.12.532249v1.full.pdf (2023).
192. Sung, J. H., Yu, J., Luo, D., Shuler, M. L. & March, J. C. Microscale 3-D hydrogel scaffold for biomimetic gastrointestinal (GI) tract model. *Lab. Chip* **11**, 389-392 (2011).
193. Silver, F. H., Freeman, J. W. & Seehra, G. P. Collagen self-assembly and the development of tendon mechanical properties. *J. Biomech.* **36**, 1529-1553 (2003).
194. Wershof, E. et al. Matrix feedback enables diverse higher-order patterning of the extracellular matrix. *PLoS Comput. Biol.* **15**, e1007251 (2019).
195. Park, D. et al. Extracellular matrix anisotropy is determined by TFAP2C-dependent regulation of cell collisions. *Nat. Mater.* **19**, 227-238 (2020).
196. Reznikov, N., Shahar, R. & Weiner, S. Bone hierarchical structure in three dimensions. *Acta Biomater.* **10**, 3815-3826 (2014).
197. Sartori, P., Geyer, V. F., Howard, J. & Jülicher, F. Curvature regulation of the ciliary beat through axonemal twist. *Phys. Rev. E* **94**, 042426 (2016).
198. Chabanon, M. & Rangamani, P. Geometric coupling of helicoidal ramps and curvature-inducing proteins in organelle membranes. *J. R. Soc. Interface* **16**, 20190354 (2019).
199. Hu, J. et al. Membrane proteins of the endoplasmic reticulum induce high-curvature tubules. *Science* **319**, 1247–1250 (2008).
200. Collado, J. et al. Tricalbin-mediated contact sites control ER curvature to maintain plasma membrane integrity. *Dev. Cell* **51**, 476-487.e7 (2019).
201. Tozluoğlu, M. & Mao, Y. On folding morphogenesis, a mechanical problem. *Philos. Trans. R. Soc. B* **375**, 20190564 (2020).
202. Martin, A. C., Kaschube, M. & Wieschaus, E. F. Pulsed contractions of an actin-myosin network drive apical constriction. *Nature* **457**, 495-499 (2009).
203. Storgel, N., Krajnc, M., Mrak, P., Štrus, J. & Ziherl, P. Quantitative morphology of epithelial folds. *Biophys. J.* **110**, 269-277 (2016).
204. Sui, L. et al. Differential lateral and basal tension drive folding of *Drosophila* wing discs through two distinct mechanisms. *Nat. Commun.* **9**, 4620 (2018).
205. Wang, Y. et al. A microengineered collagen scaffold for generating a polarized crypt-villus architecture of human small intestinal epithelium. *Biomaterials* **128**, 44-55 (2017).
206. Savin, T. et al. On the growth and form of the gut. *Nature* **476**, 57-62 (2011).
207. Huycke, T. R. et al. Genetic and mechanical regulation of intestinal smooth muscle development. *Cell* **179**, 90-105.e21 (2019).
208. Garcia, K. E., Kroenke, C. D. & Bayly, P. V. Mechanics of cortical folding: stress, growth and stability. *Philos. Trans. R. Soc. B* **373**, 20170321 (2018).
209. Callens, S. J. P. & Zadpoor, A. A. From flat sheets to curved geometries: origami and kirigami approaches. *Mater. Today* **21**, 241-264 (2018).

Acknowledgements

The authors apologize to all authors whose work could not be included owing to space constraints. S.G. acknowledges funding from FEDER Prostem Research Project no. 1510614 (Wallonia DG06), the F.R.S.-FNRS Epiforce Project no. T.0092.21, the F.R.S.-FNRS Cellsqueezer Project no. J.0061.23, the F.R.S.-FNRS Optopattern Project no. U.NO26.22, Programme Wallon d'Investissement Région Wallone pour les instruments d'imagerie (INSTIMAG UMONS #1910169) and the Interreg MAT(T)ISSE project, which is financially supported by Interreg France-Wallonie-Vlaanderen (Fonds Européen de Développement Régional, FEDER-ERDF). M.L. is financially supported by a WBI.World Scholarship Fellowship from the Wallonia-Brussels International (WBI) Excellence Grants Programme. A.R. acknowledges funding from the Swiss National Fund for Research Grants nos 31003A_149975, 31003A_173087 and 31003A_200793, and the European Research Council Synergy Grant no. 951324_R2-TENSION. The authors want to thank the NCCR Chemical Biology for constant support during this project. C.T. acknowledges support from the French National Research Agency, Grant no. ANR-22-CE13-0015-01 for the project 'CurvEDyn'.

Author contributions

M.L., C.T., A.R. and S.G. conceptualized the article. Figure designs were generated by all authors and further edited by M.L. and S.G. All authors contributed substantially to the writing, the discussion of the content and approved the final content.

Competing interests

The authors declare no competing interests.

Additional information

Peer review information *Nature Reviews Physics* thanks Krisopher Kilian, Tsuyoshi Hirashima and the other, anonymous, reviewer(s) for their contribution to the peer review of this work.